



Université de Montréal

**Rat protease-activated receptor-1 (rPAR1) expression and characterization in Sf9 cells**

par

Maria Lavalle

Département de physiologie moléculaire et intégrative  
Faculté de Médecine

Mémoire présenté à la Faculté de Médecine  
en vue de l'obtention du grade de Maître ès sciences (M.Sc.)  
en physiologie moléculaire, cellulaire et intégrative

juillet 2014  
©Maria Lavalle, 2014

Université de Montréal  
Faculté de Médecine

Ce mémoire intitulé:

**Rat protease-activated receptor - 1(rPAR1) expression and characterization in Sf9 cells**

Présenté par:

Maria Lavalle

a été évalué par un jury composé des personnes suivantes :

Dr Réjean Couture (Ph.D.)  
Président-rapporteur

Dr Madhu Anand-Srivastava (Ph.D.)  
Membre du jury

Dr Jean-Louis Schwartz (Ph.D.)  
Directeur de recherche

*To my family,  
for their continual encouragement and support.  
And to my research director,  
for his guidance, generosity and friendship*

## RÉSUMÉ

Connue pour son rôle dans la cascade de coagulation, la thrombine, une protéase à sérine, peut également agir par l'intermédiaire de PAR1, un récepteur activé par protéase et couplé aux protéines G liant le GTP (GPCR). La thrombine se lie et clive l'extrémité N-terminale du PAR1 entre l'Arg<sup>41</sup> et la Ser<sup>42</sup>, exposant une nouvelle extrémité terminale qui agit elle-même comme un ligand. La thrombine et une séquence peptidique de cinq acides aminés, composée des résidus Ser<sup>42</sup> à Arg<sup>46</sup>, nommée PAR1-AP, déclenchent dans diverses cellules de mammifères une réponse intracellulaire comportant une composante calcique.

Dans cette étude, le système d'expression par baculovirus dans les cellules Sf9 d'insecte nous a permis d'exprimer le récepteur PAR1 du rat à la surface de ces cellules et de réaliser son couplage fonctionnel à leur signalisation intracellulaire (modèle rPAR1-Sf9). La composante calcique de celle-ci, en réponse au PAR1-AP, a ensuite été étudiée en détail à l'aide de la sonde fluorescente Fura-2 et de plusieurs inhibiteurs agissant sur les canaux calciques ou d'autres éléments de la cascade de signalisation du calcium intracellulaire.

Lorsque le milieu extracellulaire contient du calcium ( $\text{Ca}^{2+}$ ), la thrombine ou PAR1-AP déclenchent un signal calcique qui consiste en une augmentation rapide de  $[\text{Ca}^{2+}]_i$  suivi d'un plateau relativement soutenu, puis d'un retour lent vers le niveau de base initial. En l'absence de  $\text{Ca}^{2+}$  dans le milieu extracellulaire, l'augmentation initiale rapide de  $[\text{Ca}^{2+}]_i$  est suivie d'un retour rapide vers le  $[\text{Ca}^{2+}]_i$  de base.

À l'aide d'inhibiteurs de canaux calciques, tels que le lanthane, la nifédipine et le D-600, l'entrée du calcium du milieu extracellulaire dans les cellules est inhibée, abolissant le plateau soutenu de  $[\text{Ca}^{2+}]_i$ . L'inhibition de la pompe  $\text{Ca}^{2+}$ -ATPase par la thapsigargine supprime la réponse au PAR1-AP après épuisement des sites de stockage de

$\text{Ca}^{2+}$  intracellulaire. Le TMB-8 agit de façon discordante quant à l'inhibition de la libération de  $\text{Ca}^{2+}$  des sites de stockage intracellulaires. La réponse à PAR1-AP n'est pas affectée par le D-609, un inhibiteur de la phospholipase  $\beta$ . L'inhibition de la protéine kinase C (PKC) par le bisindolylmaléimide induit des oscillations en présence de  $\text{Ca}^{2+}$  extracellulaire et atténue fortement le signal calcique en absence de  $\text{Ca}^{2+}$  extracellulaire. En présence de  $\text{Ca}^{2+}$  extracellulaire, l'activation de la PKC par le PBDu tronque le flux de  $[\text{Ca}^{2+}]_i$ ; tandis que la réponse calcique est abolie en absence de  $\text{Ca}^{2+}$  dans le milieu extracellulaire. Le H-89, un inhibiteur de la protéine kinase A (PKA), cause une prolongation de la durée du plateau de  $[\text{Ca}^{2+}]_i$  dans un milieu riche en calcium et la suppression de la réponse à PAR1-AP lorsque le milieu extracellulaire est dépourvu de  $\text{Ca}^{2+}$ .

Les résultats obtenus nous permettent de conclure que la PKC et possiblement la PKA jouent un rôle critique dans la mobilisation du  $\text{Ca}^{2+}$  induite par le PAR1-AP dans le modèle rPAR1-Sf9.

**Mots clés:** cellule Sf9, baculovirus, thrombine, récepteur activé par protéase (PAR), signalisation calcique, canal calcique, Fura-2

## ABSTRACT

Thrombin's serine protease activity allows for it to have a role in both the coagulation cascade as well as through a GTP-binding protein coupled receptor (GPCR) known as the protease-activated receptor-1 (PAR1). Thrombin binds to PAR1 at the N-terminal, cleaving between Arg<sup>41</sup> and Ser<sup>42</sup>, and unmasking a new N-terminal which acts as a tethered ligand. Thrombin and a five amino acid peptide composed of the sequence of residues Ser<sup>42</sup> to Arg<sup>46</sup>, known as PAR 1-AP, has been shown to mediate a number of signalling mechanisms in mammalian cells, including a calcium signalling pathway.

In the present study, the Sf9-baculovirus system allowed us to express the rat PAR1 (rPAR1-Sf9) on the cell surface and study its intracellular signalling. The calcium (Ca<sup>2+</sup>) signal was studied using the fluorescent probe Fura-2, and several Ca<sup>2+</sup> channel inhibitors and calcium signal modulators were used to study the signal induced by PAR1-AP.

In the presence of extracellular calcium [Ca<sup>2+</sup>]<sub>e</sub>, thrombin and PAR1-AP produced a Ca<sup>2+</sup> signal which consisted of an initial spike in [Ca<sup>2+</sup>]<sub>i</sub> followed by a relatively maintained plateau and a slow return towards baseline. In the absence of Ca<sup>2+</sup> in the extracellular space, the initial Ca<sup>2+</sup> increase is followed by a quick return to baseline [Ca<sup>2+</sup>]<sub>i</sub>.

Ca<sup>2+</sup> channel inhibitors, lanthanum, nifedipine and D-600, inhibited the entry of Ca<sup>2+</sup> from the extracellular space and abolished the plateau phase of the response to PAR1-AP. Inhibition of the Ca<sup>2+</sup>-ATPase with thapsigargin abolished the response to PAR1-AP after having depleted the Ca<sup>2+</sup> stores involved in the initial spike in [Ca<sup>2+</sup>]<sub>i</sub>. TMB-8, expected to inhibit the release of Ca<sup>2+</sup> from internal stores, inconsistently inhibited the [Ca<sup>2+</sup>]<sub>i</sub> response to PAR1-AP. The response elicited by PAR1-AP was not affected by D-609, an inhibitor of phospholipase C $\beta$ . Inhibition of protein kinase C (PKC) with bisindolylmaleimide induced

oscillations in the  $[Ca^{2+}]_i$  levels in the presence of extracellular  $Ca^{2+}$  while it significantly blunted the response in the absence of extracellular  $Ca^{2+}$ . PDBu activation of PKC truncated the  $[Ca^{2+}]_i$  surge in  $Ca^{2+}$ -rich conditions while abolishing it altogether in the absence of extracellular  $Ca^{2+}$ . H-89 inhibition of protein kinase A (PKA) prolonged the plateau duration in  $Ca^{2+}$ -rich medium while inhibiting the response to PAR1-AP in a  $Ca^{2+}$ -deficient environment.

Taken together, our results suggest that PKC and possibly PKA play a critical role in the mobilisation of  $Ca^{2+}$  in rPAR1-Sf9 by PAR1-AP.

**Key words:** Sf9, baculovirus, thrombin, protease-activated receptor (PAR), calcium signalling, calcium channel, Fura-2.



## TABLE OF CONTENTS

<b>DEDICATION</b> .....	<b>iii</b>
<b>RÉSUMÉ</b> .....	<b>iv</b>
<b>LIST OF FIGURES</b> .....	<b>x</b>
<b>LIST OF TABLES</b> .....	<b>xi</b>
<b>ABBREVIATIONS</b> .....	<b>xii</b>
<b>ACKNOWLEDGEMENTS</b> .....	<b>xiv</b>
<b>INTRODUCTION</b> .....	<b>1</b>
<b>1.1 Coagulation cascade</b> .....	<b>2</b>
<b>1.2 Thrombin and its receptor</b> .....	<b>3</b>
1.2.1 Thrombin .....	3
1.2.2 Protease-activated receptor 1 (PAR1) .....	4
1.2.3 PAR1-mediated role of thrombin .....	8
<b>1.3 Protease-activated receptor 1 (PAR1) activation</b> .....	<b>10</b>
1.3.1 G-protein coupling to PAR1 and signalling cascade in mammalian cells .....	10
1.3.2 Focus on Ca <sup>2+</sup> mobilisation and store-operated Ca <sup>2+</sup> entry (SOCE) .....	12
1.3.3 Inactivation of the receptor .....	14
1.3.4 Recent advances in understanding PARs .....	15
<b>1.4 Spodoptera frugiperda (Sf9) cell line</b> .....	<b>16</b>
<b>1.5 Rationale, hypothesis and objectives</b> .....	<b>18</b>
<b>MATERIALS AND METHODS</b> .....	<b>20</b>
<b>2.1 Construction of the recombinant baculovirus rPAR1 and virus preparation</b> .....	<b>21</b>
<b>2.2 Infection procedure</b> .....	<b>22</b>
<b>2.3 Detection of expressed receptor in cell membranes</b> .....	<b>22</b>
2.3.1 Receptor–antibody cross-linking studies in rPAR1-Sf9 cells.....	22
2.3.2 Western blot membrane preparation and endoglycosidase treatment of rPAR1 .....	23
2.3.3 Immunocytochemistry, fluorescence-activated cell sorting (FACS) and confocal microscopy .....	25
<b>2.4 Functional assays</b> .....	<b>26</b>
2.4.1 Solutions .....	26

2.4.2 Preparation and use of agonists and signal modulators .....	27
2.4.3 Microspectrofluorescence.....	28
<b>RESULTS. ....</b>	<b>30</b>
<b>3.1 Sf9-baculovirus expression system of rPAR1 receptor .....</b>	<b>31</b>
3.1.1 Successful expression of rPAR1 .....	31
3.1.2 Localization of the rPAR1 receptor expressed in Sf9 cells .....	32
<b>3.2 Changes in [Ca<sup>2+</sup>]<sub>i</sub> concentration using octopamine.....</b>	<b>34</b>
<b>3.3 Functional coupling of rPAR1 in Sf9 cells.....</b>	<b>38</b>
3.3.1 Effect of thrombin .....	38
3.3.2 Effect of PAR1-AP .....	39
<b>3.4 Modulation of the rPAR1-Sf9 cell signal .....</b>	<b>41</b>
3.4.1 Effect of calcium-channel inhibitors .....	41
3.4.2 Effect of other calcium transport modulators .....	45
3.4.3 Signal cascade modulation .....	48
<b>DISCUSSION.....</b>	<b>53</b>
<b>4.1 Sf9-Baculovirus expression system.....</b>	<b>54</b>
<b>4.2 Effective coupling of rPAR1 and modulation of response in Sf9 cells.....</b>	<b>56</b>
<b>4.3 Store-operated Ca<sup>2+</sup> entry .....</b>	<b>62</b>
<b>CONCLUSION AND FUTURE DIRECTIONS.....</b>	<b>66</b>
<b>5.1 Conclusion .....</b>	<b>67</b>
<b>5.2 Future directions.....</b>	<b>68</b>
<b>APPENDIX. Calibration of Ca<sup>2+</sup> concentration .....</b>	<b>69</b>
<b>BIBLIOGRAPHY.....</b>	<b>72</b>

## LIST OF FIGURES

### INTRODUCTION

Figure 1: Thrombin's molecular structure.....	4
Figure 2: Structure of human PAR1 with an antagonist.....	5
Figure 3: PAR1 sequence.....	6
Figure 4: Thrombin binding to PAR1 exodomain.....	8
Figure 5: PAR1 signalling cascade activation.....	10

### RESULTS

Figure 6: Western blot analysis of rPAR1 infected Sf9 cells.....	32
Figure 7: FACS analysis of rPAR1 expression.....	33
Figure 8: Different views of confocal micrographs of a single Sf9 cell expressing rPAR1.....	34
Figure 9: Effect of octopamine on cytosolic calcium in wild-type Sf9 cells.....	35
Figure 10: Effect of infection time on intracellular Ca <sup>2+</sup> concentration change in response to octopamine in baculovirus-Sf9 cells.....	36
Figure 11: Effect of thrombin on [Ca <sup>2+</sup> ] <sub>i</sub> in Sf9 insect cells expressing rPAR1.....	39
Figure 12: Effect of synthetic peptide PAR1-AP on [Ca <sup>2+</sup> ] <sub>i</sub> in rPAR1-Sf9 cells.....	40
Figure 13: Effect of La <sup>3+</sup> pre-incubation on the [Ca <sup>2+</sup> ] <sub>i</sub> response to PAR1-AP.....	42
Figure 14: Effect of La <sup>3+</sup> applied during the [Ca <sup>2+</sup> ] <sub>i</sub> surge triggered by PAR1-AP.....	43
Figure 15: Effect of nifedipine on the Ca <sup>2+</sup> flux produced by PAR1-AP activation in rPAR1-Sf9 cells.....	44
Figure 16: Effect of D-600 on the [Ca <sup>2+</sup> ] <sub>i</sub> response to PAR1-AP.....	45
Figure 17: Effect of thapsigargin on the [Ca <sup>2+</sup> ] <sub>i</sub> response to PAR1-AP activation in rPAR1-Sf9.....	46
Figure 18: TMB-8 inhibition of Ca <sup>2+</sup> release from the ER.....	47
Figure 19: Ineffective inhibition by TMB-8.....	47
Figure 20: Effect of D-609 on the [Ca <sup>2+</sup> ] <sub>i</sub> response to PAR1-AP.....	49
Figure 21: Effect of bisindolylmaleimide on the [Ca <sup>2+</sup> ] <sub>i</sub> response induced by PAR1-AP...	50
Figure 22: Effect of PDBu on the Ca <sup>2+</sup> surge produced by PAR1-AP.....	51
Figure 23: Effect of H-89 on the [Ca <sup>2+</sup> ] <sub>i</sub> response to PAR1-AP.....	52
Figure 24: Ca <sup>2+</sup> signal modulation in rPAR1-Sf9.....	58

### APPENDIX 1

Figure 25: Calcium signal calibration.....	70
--	----

## LIST OF TABLES

Table 1: Summary of qualitative changes in Fura-2 fluorescence ratio reflecting $[Ca^{2+}]_i$ in control experiments.....	37
---	----

## ABBREVIATIONS

AC	adenylyl cyclase
AcMNPV	<i>Autographa californica</i> nuclear polyhedrosis virus
ADP	adenosine diphosphate
Arg	arginine
Asp	aspartic acid
ATP	adenosine triphosphate
$\beta$ ARK2	beta-adrenergic receptor kinase - 2
BSA	bovine serum albumin
BS3	bis (sulfosuccinimidyl) suberate
$\text{Ca}^{2+}$	calcium ion
$[\text{Ca}^{2+}]_i$	intracellular calcium concentration
$[\text{Ca}^{2+}]_e$	extracellular calcium concentration
cDNA	complementary deoxyribonucleic acid
$\text{Cl}^-$	chloride ion
D-600	methoxyverapamil
D-609	tricyclodecan-9-yl xanthogenate
DAG	diacylglycerol
DNA	deoxyribonucleic acid
DTS	dense tubular system
EGTA	ethylene-glycotetraacetic acid
ER	endoplasmic reticulum
FACS	fluorescence-activated cell sorter
FBS	fetal bovine serum
F	fluoride
GEF	guanine exchange factor
GPRC	GTP-binding protein coupled receptor
GSM	Grace's simplified medium
h	hour
$\text{H}^+$	hydrogen ion
$\text{H}_2\text{O}$	water
H-89	N-[2-[[3-(4-bromophenyl)-2-propenyl]amino]ethyl]-5-1 isoquinolinesulfonamide
Ig	immunoglobulin
$\text{IP}_3$	inositol 1,4,5 triphosphate
$\text{K}^+$	potassium ion
$\text{La}^{3+}$	lanthanum ion
Leu	leucine
M3	muscarinic receptor 3
M5	muscarinic receptor 5
MAP	mitogen-activated protein
MAPK	mitogen-activated protein kinase
MOI	multiplicity of infection
Na	sodium ion

NCCE	non-capacitative Ca <sup>2+</sup> entry
nm	nanometer
PAF	platelet activating factor
PAR	protease-activated receptor
PAR1	protease-activated receptor-1
PAR2	protease-activated receptor-2
PAR3	protease-activated receptor-3
PAR4	protease-activated receptor-4
PBS	phosphate buffered saline
PCR	polymerase chain reaction
PDBu	phorbol 12, 13-dibutyrate
Phe	phenylalanine
PI3K	phosphoinoside 3-kinase
PIP <sub>2</sub>	phosphatidylinositol 4,5-biphosphate
PK	protein kinase
PKA	protein kinase A
PKC	protein kinase C
PLC	phospholipase C
PLD	phospholipase D
Pro	proline
RNA	ribonucleic acid
rpm	revolutions per minute
RT-PCR	reverse transcriptase – polymerase chain reaction
s	seconds
SDS-PAGE	sodium dodecyl sulphate –polyacrylamide gel electrophoresis
Ser	serine
Sf	<i>Spodoptera frugiperda</i>
SOC	store-operated calcium channel
SOCE	store-operated calcium entry
SRE	sterol responsive element
STIM-1	stromal interaction molecule-1
TB	tris (hydroxymethyl) aminomethane buffer
TMB-8	3,4,5-trimethoxybenzoic acid 8-(diethylamino)octyl ester
Tris	tris (hydroxymethyl) aminomethane
V	volts
X-gal	5-bromo-4-chloro-3-indolyl-beta-D-galacto-pyranoside

## **ACKNOWLEDGEMENTS**

A very special note of gratitude to my director, Dr Jean-Louis Schwartz, for his guidance and counsel throughout this process. Your continuous support was instrumental to the realization of this work.

To the jury members, Dr Rejean Couture and Dr Madhu Anand-Srivastava, a sincere thank you for your comments and suggestions in rendering this document final.

I would also like to thank the National Research Council of Canada and the staff at the Biotechnology Research Institute, including Dr Maureen O'Connor-McCourt and her staff, most notably Cathy Collins for her help in building the recombinant baculovirus.

As well, many thanks to Roseanne Tom, Léna Potvin and Narcisse Komars for their aid on various aspects of cell culture, microspectrofluorescence and confocal microscopy.

I would also like to thank Dr Morley D. Hollenberg, for his collaboration on designing this study, and his group for providing the antibodies used throughout the study.

A special acknowledgement to Dr Martin Noel and Dr Paul Poirier for the enthusiasm with which they provided editorial support.

Special thanks to the Canadian Institutes of Health Research for providing funding for this project through a collaborative research grant to M.H. and J.L.S. and Biochem Pharma.

A particular thank you to AstraZeneca Canada for providing an environment whereby learning and development are encouraged as part of the corporate culture.

Finally, I would like to thank every member of my family, especially my parents, my husband Mike and our children (Anthony, Tessa-Marie, Joel and Kiara), for their love, support and encouragement over the course of this process.

# **INTRODUCTION**



Thrombin is a well-studied protein of the coagulation cascade. Its proteolytic activity has long interested cardiovascular physiologists, due to its critical involvement in the formation of platelet plugs and subsequent clot formation. The proteolytic cleavage of fibrinogen to fibrin, by thrombin, is a critical step in clot stabilization. It is now known that thrombin's actions go well beyond the cleavage of fibrinogen. Thrombin is involved in the pathophysiology of thrombosis, and in other processes including atherosclerosis [1], and even tumor growth [2].

By studying thrombin's effects on different functional systems, investigators identified the thrombin receptor [3] as part of a unique subclass of G-protein coupled receptor (GPCR), activated through proteolytic cleavage of the extracellular domain. The subclass is known as the protease activated receptors (PARs). While thrombin's serine protease action is a critical component of the coagulation cascade, activation of its receptor, the protease activated receptor-1 (PAR1), mediates much of thrombin's cellular activity [2, 4-7].

## **1.1 Coagulation cascade**

The coagulation cascade is integral to maintaining homeostasis and is divided into an intrinsic and an extrinsic system.

The intrinsic pathway, is activated by the exposure of subendothelial collagen, platelet phospholipids and the presence of ionized calcium and plays a secondary role in coagulation.

The extrinsic system is the principal pathway of blood coagulation. It involves both vascular and blood elements. Vascular injury damages endothelial cells and exposes tissue factor; a glycoprotein embedded in and around blood vessels and various other tissue cells. Tissue factor contributes to the activation of the extrinsic pathway of the coagulation cascade, which begins with an inactive form of Factor VII. A series of steps ensues whereby each

coagulation factor is activated by its predecessor [8], with the exception of those factors that are involved in the common pathway.

Lastly, blood components, in particular, leukocyte and monocyte derived microparticles, can be recruited to sites of vascular injury, and express low levels of tissue factor as well, thus play a role in activating the coagulation cascade.

The common pathway refers to the final steps of the coagulation cascade common to both the intrinsic and extrinsic systems and consists of the activation of Factor X to form Factor Xa. This critical step is required for the cleavage of thrombin from its precursor state, prothrombin [9].

Thrombin is ultimately required for the cleavage of fibrinogen into fibrin through its serine protease activity. This final step in the coagulation cascade is responsible for clot stabilization and solidification [9].

## **1.2 Thrombin and its receptor**

### **1.2.1 Thrombin**

While thrombin is best known for its role in the circulatory system, it has also been identified as being involved in a multitude of different physiological systems including the vascular, respiratory, gastrointestinal, renal, musculoskeletal and nervous systems [6].

Within the circulatory system, inappropriate activation of thrombin leads to the formation of thrombi. These circulating blood clots may partially or fully occlude blood vessels, causing thrombosis, stroke or cardiac ischemia.

Thrombin's structure consists of a globular protein (Figure 1A), composed of two chains which are 36 and 259 amino acids in length and linked by a single disulfide bond. It is

ellipsoid in shape and interacts with its substrates in a highly specific manner [7]. The structural details of this interaction are shown in Figure 1B.

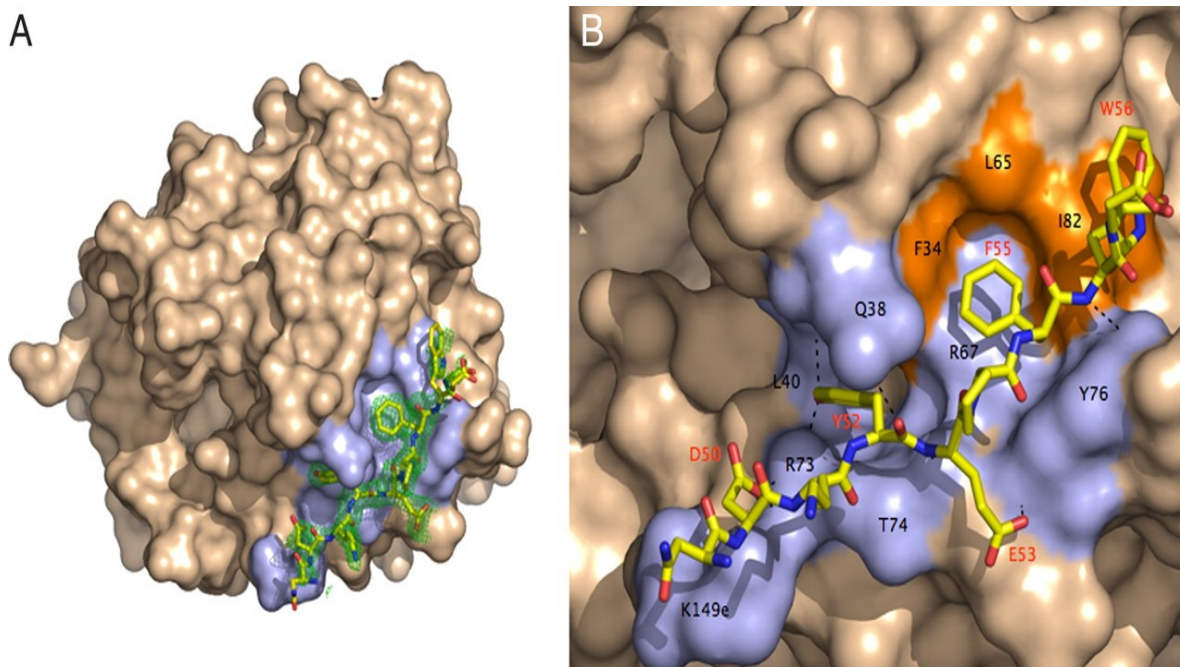


**Figure 1: Thrombin’s molecular structure. A: Thrombin structure.** Thrombin’s active site is flanked by three catalytic amino acids (His<sup>43</sup>, Asp<sup>99</sup>, Ser<sup>205</sup>) at its base. This triad is surrounded by the primary specificity pocket (Asp<sup>109</sup>) and two insertion loops [10]. Two anion binding exosites are located at the extremities of the molecule and are responsible for thrombin’s actions. Anion exosite 1 recognizes fibrinogen and the N-terminal of PAR1, while exosite 2 is involved in the interaction with heparin [11]. **B: Thrombin–PAR1 interface.** The hydrophobic regions of thrombin are coloured in orange and its polar regions are light blue. Thrombin’s residues involved in contact with PAR1 sit in the hydrophobic region with black labels representing thrombin’s residues and red labels representing the residues located on PAR1. The residues involved in the cleavage of the extracellular fragment of PAR1 have been labelled in red. The N-terminal of PAR1 fits into exosite 1 through polar and hydrophobic interactions. Hydrogen bonds which form between thrombin and PAR1 are depicted as broken lines [10]. (*Adapted from* [10])

### 1.2.2 Protease-activated receptor 1 (PAR1)

In addition to its role in the coagulation cascade, thrombin exerts its receptor-specific activity through PAR1 [6]. The PAR1 receptor is a member of the GPCR receptor

superfamily. The three-dimensional structure of the human PAR1 crystalized in the presence of vorapaxar, a PAR1 antagonist, has recently been elucidated [12] and is shown in Figure 2.

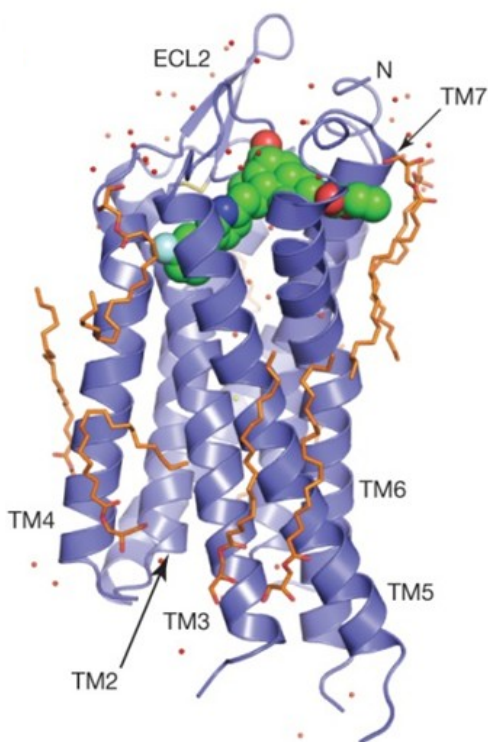


**Figure 2: Structure of human PAR1 with an antagonist.** The overall structure of PAR 1 is shown with transmembrane helices labelled TM2-7. Extracellular loop 2 (ECL2) and the N-terminal (N) of the receptor are critical components of the receptor activation by the tethered ligand. Orange sticks represent lipid molecules required for crystallogenesi technique and may not be present in actual physiological conditions. The antagonist (vorapaxar) is represented in green. (*Adapted from [13]*)

The protein is 425 amino acids long, and is organized into seven helical transmembrane domains with three intracellular and three extracellular loops (Figure 2 and Figure 3A). The N-terminal of the receptor is extracellular. This exodomain contains the thrombin cleavage site and the region that will form the new ligand after cleavage. Figure 3B shows the primary sequences of the human, mouse, hamster and rat PAR1 exodomains, as well as the tethered ligand sequences, the thrombin interaction sites and the ligand binding sites. They display a high level of homology. The C-terminal of PAR1 is located intracellularly and possesses a large number of serine and threonine residues.

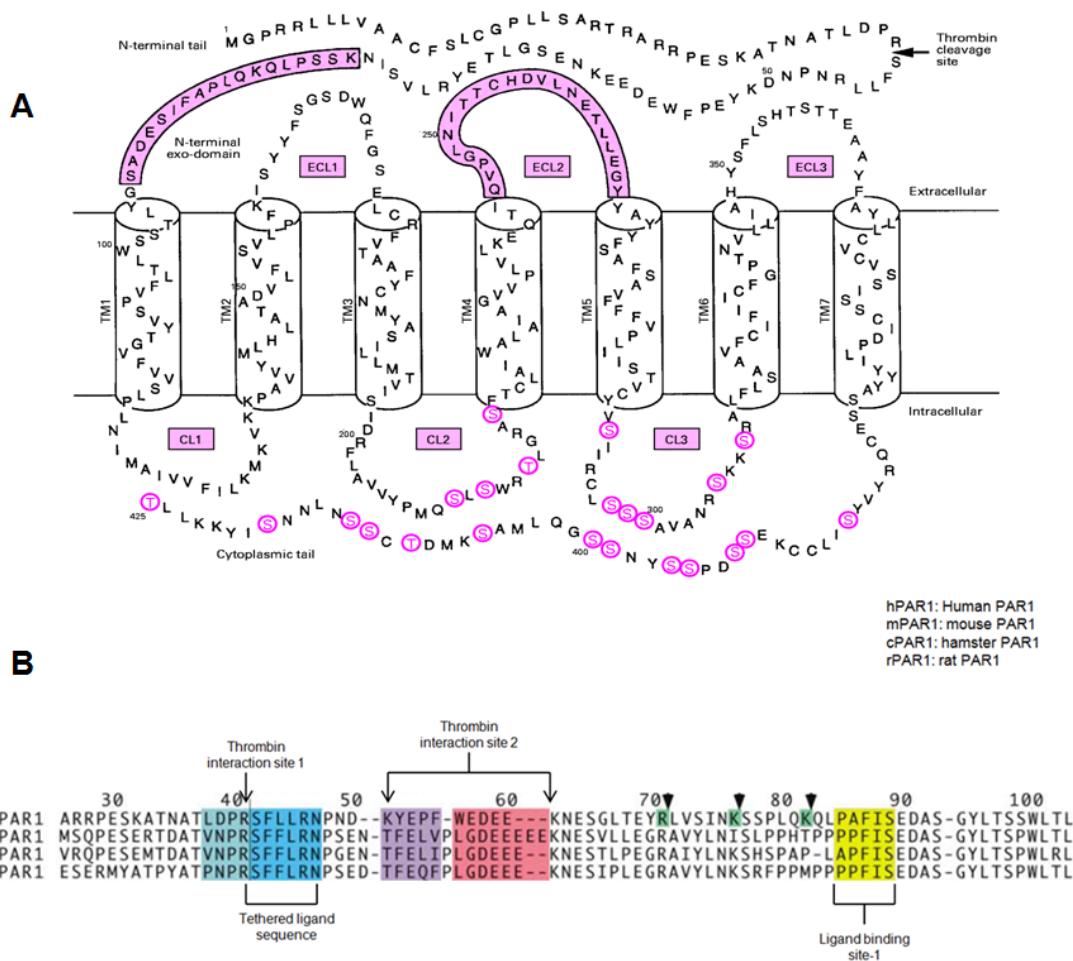


**Figure 3: A: PAR1 sequence.** The amino acid sequence includes the thrombin cleavage site, the extracellular domain, extracellular loops (ECL) and cytoplasmic loops (CL). Intracellular phosphorylation sites appear in red letters. Pink boxes include the extracellular domains where the newly cleaved N-terminal interacts with the ligand binding site-1 (located in the N-terminal exodomain above) and extracellular loop 2 (ECL2). (*Adapted from* [14]) **B. PAR1 exodomain sequences in various species.** Considerable sequence homology exists in PAR1 exodomains across species. Thrombin molecules interact with the receptor through thrombin interaction sites 1 and 2. Cleavage of the peptide bond between Arg<sup>41</sup> and Ser<sup>42</sup> yields a new N-terminal. The peptide sequence located at the new N-terminal is referred to as the tethered ligand sequence. The receptor's N-terminal binds at ligand binding site-1 to activate downstream signalling. (*Adapted from* [15])

Thrombin activates its receptor through a highly specific ( $K_m$  of 15-30  $\mu$ M) proteolytic cleavage at a site located between residues Arg<sup>41</sup> and Ser<sup>42</sup> (Figure 3) [15-17]. Thrombin's receptor mediated activity depends on its ability to bind to the PAR1 receptor's N-terminal

exodomain (Figure 4) and cleave a peptide bond between Arg<sup>41</sup> and Ser<sup>42</sup>, yielding a new N-terminal [9].

Receptor activation occurs through two thrombin interaction sites on the receptor; the first immediately N-terminal to Arg<sup>41</sup> and the second between residues 53 (responsible for the recognition of the receptors' cleavage site) and 64 (involved in an interaction with one of the anion binding exosites on thrombin). PAR1 requires interaction of the Arg-Asp-Pro-Leu segment with the apolar pocket of the thrombin molecule [18]. In the interaction of thrombin with its receptor, an initial contact is made between exosite-1 (Figure 4) on thrombin and the receptor's thrombin interaction site-1 (Figure 3B). The N-terminal then becomes newly oriented, and a hydrogen bond between Asp<sup>39</sup> and Arg<sup>41</sup> is disrupted, freeing the arginine and allowing cleavage of the receptor to occur through thrombin's active site (Figure 3) [14, 15]. Cleavage creates a new, tethered, N-terminal sequence starting after Arg<sup>41</sup>, which binds to the ligand binding site-1 [15] located within the N-terminal exodomain [19]. Although extracellular loop 2 is the main site for binding of the tethered ligand (Figure 3A), binding also involves domains present on extracellular loop 1 as well as on extracellular loops 3 and 4 [15].

Synthetic peptides corresponding to the new N-terminal sequence have been shown to activate the receptor, generating downstream signals in mammalian cells [15, 20]. While the tethered ligand sequences shown in Figure 3B are made up of six amino acids ending with Asp, a minimal peptidomimetic compound, PAR1-activating peptide (PAR1-AP), corresponds to the five amino acids, Ser-Phe-Leu-Leu-Arg, that immediately follow the cleavage site.

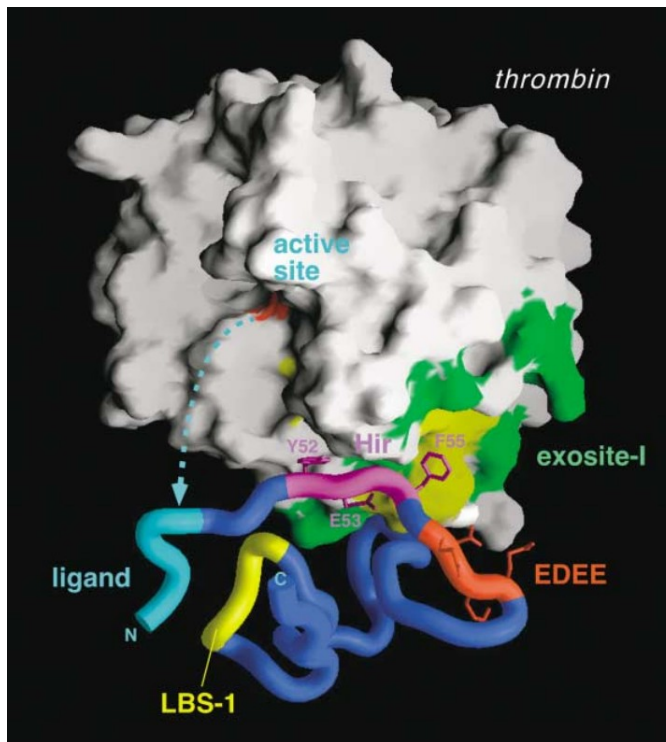


**Figure 4: Thrombin binding to PAR1 exodomain.** The globular protein thrombin binds to the exodomain of the PAR1 through polar and hydrophobic interactions. The extremity of the N-terminal fits into thrombin's active site where it is cleaved, yielding a new N-terminal (denoted as N in figure) which acts as a tethered ligand. The tethered ligand (marked ligand in figure) can then activate cell signalling through an interaction with another area of the exodomain labelled ligand binding site-1 (LBS-1). The minimal peptidic sequence known to activate PAR1 corresponds to the five amino acid sequence Ser-Phe-Leu-Leu-Arg. (*adapted from [15]*)

### 1.2.3 PAR1-mediated role of thrombin

The thrombin receptor was the first PAR to be identified in its subclass, which is the reason for it having been named PAR1. It is a well-studied member of the PAR superfamily. Genetic and physical mapping of this receptor led to the recognition of additional protease-activated receptor subtypes, including PAR2 [21], PAR3 [22], and PAR4 [23]. While PAR1, PAR3 and PAR4 are activated by thrombin, PAR2 is activated by the Tissue Factor/VIIa binary complex and by Factor Xa [6]. While mostly colocalized within 90kb of each other on

chromosome 5q13 [24], the human PAR4 gene is located on chromosome 19p12 [25]. PARs are often co-expressed and coactivation has been identified as a mechanism of action for some PARs in *in-vitro* testing [5].

For the purpose of this work, focus will be placed on PAR1, the first receptor identified in the PAR-superfamily.

As thrombin results from the cleavage of prothrombin in the circulatory system, it is intuitive to deduce that blood components would be amongst the key targets of thrombin. In particular, the PAR1 receptor plays a substantial role in platelet activation, particularly at low thrombin concentrations [8]. PAR1 activation in platelets is associated with platelet shape change, aggregation and granular secretion responsible for hemostasis which involves adenosine diphosphate (ADP), 5-hydroxytryptamine [26], platelet activating factor (PAF), and thromboxane [9]. Platelet shape change results in increased platelet adhesion to exposed tissues. Platelet degranulation serves to amplify platelet aggregation. Activation of the platelet increases the cell-surface expression of glycoproteins IIb/IIIa – a fibrin cross-linking site essential for clot solidification.

The inappropriate activation of platelets through the action of PAR1 can lead to serious medical conditions caused by the formation of thrombi, including myocardial infarct and stroke. For this reason, PAR1 has the potential to be a useful pharmacological target. Zontivity™ (vorapaxar) which has been approved by the US Food and Drug Administration in May 2014 is the first pharmaceutical antagonist of PAR1.

([www.fda.gov/NewsEvents/Newsroom/PressAnnouncements/ucm396585.htm](http://www.fda.gov/NewsEvents/Newsroom/PressAnnouncements/ucm396585.htm), 8/5/2014).

In addition to its expression on platelets, PAR1 is also expressed on other cells. For example, macrophages [27], endothelial cells [7] and vascular smooth muscle cells [1] have all



been shown to express PAR1 and are involved in a thrombin-mediated response to vascular injury [6].

### 1.3 Protease-activated receptor 1 (PAR1) activation

#### 1.3.1 G-protein coupling to PAR1 and signalling cascade in mammalian cells

The subtype of G-protein activated by a given receptor depends upon the transmembrane segments of receptors in concert with the cytoplasmic loops [28]. In the case of PAR1, coupling occurs in a promiscuous fashion with multiple G-protein families:  $G_{\alpha_{12/13}}$  [29],  $G_{\alpha_q}$  [9] and  $G_{\alpha_{i/z}}$  [8], thus allowing for modulation of a number of intracellular signalling pathways, as described below and represented schematically in Figure 5. The first of these,  $G_{\alpha_{12/13}}$ , modulates shape change, the initial phase of platelet activation. The  $\alpha_{12/13}$  subunit activates myosin light-chain phosphatases via Rho-guanine exchange factors (GEFs), activated Rho (small G-protein) and Rho-activated kinases. In some nucleated cells, this pathway mediates the function of cadherins, catenins and sterol-responsive element (SRE) required for permeability and migration in endothelial cells [9].

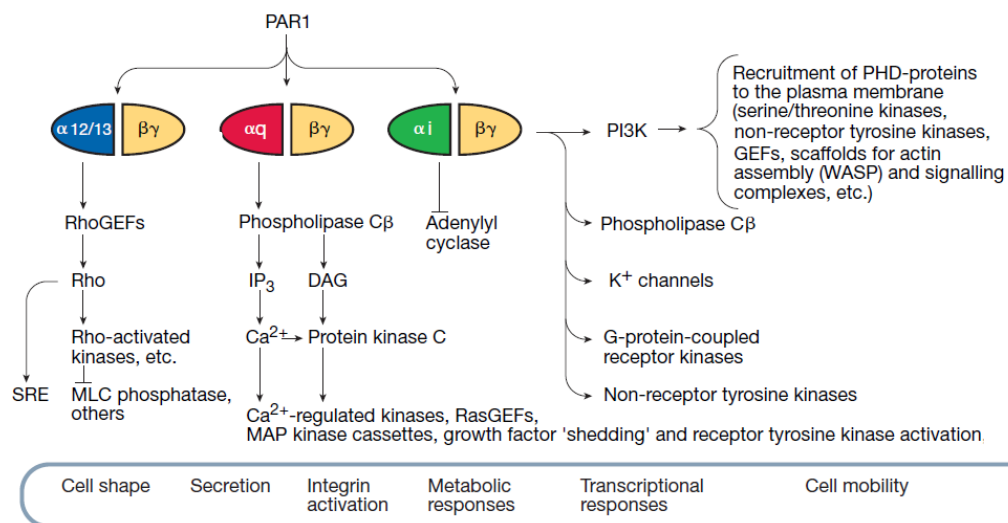


**Figure 5: PAR1 signalling cascade activation.** The figure shows the downstream signalling cascades activated by the thrombin receptor in mammalian cells. (Adapted from [9])

The G $\beta\gamma$  subunits can activate phosphoinositide 3-kinase (PI3-kinase), phospholipase C $\beta$  (PLC $\beta$ ), K $^{+}$ -ion channels, and GPCR-kinases and non-receptor tyrosine kinases [9].

G $\alpha_q$  coupling with PAR1 activates PLC $\beta$  and is primarily responsible for the formation of inositol 1,4,5-triphosphate (IP $_3$ ) and diacylglycerol (DAG), the by-products of hydrolysis of phosphatidylinositol 4,5-bisphosphate (PIP $_2$ ) [30]. Increased intracellular IP $_3$  causes Ca $^{2+}$  mobilization from its intracellular stores, activation of plasma membrane Ca $^{2+}$  channels, and activation of Ca $^{2+}$  kinases including PKC, tyrosine kinases, mitogen-activated protein kinases (MAPKs) and RasGEFs [4].

DAG activates the protein kinase C (PKC) pathway. PKC's activation mediates MAPKs, RasGEFs, Ca $^{2+}$  activated kinases and receptor tyrosine kinases. The substrates of these kinase reactions are also part of the Ras/MAPK cascade, thereby acting to enhance the initial response further and act as a feedback mechanism which terminates the activation of the signalling cascade [14]. In human platelets, a store-independent, non-capacitative Ca $^{2+}$  entry (NCCE) pathway activated by DAG has been identified as a contributor to the thrombin-induced increase in [Ca $^{2+}$ ] $_i$  [31].

The PLC $\beta$  substrate pool is replenished via PI3-kinase activity. Phosphorylation of pp125 $^{FAK}$ , through the stimulation of Rho by the G $\alpha$  subunit will precipitate pp125 $^{FAK}$  binding to Src, which will also initiate downstream signalling and PI3K activation [14], thereby allowing for the DAG pathway to complement the actions of the IP $_3$  pathway.

Phospholipase D (PLD) activity can also be secondary to thrombin's activation of PLC $\beta$  through phosphatidylinositol 4,5-bisphosphate and low molecular mass G-proteins (not shown in Figure 5). PLD catalyzes the formation of phosphatidate from phosphatidylcholine

which is responsible for the production of arachidonic acid in platelets [14] which leads to platelet activation.

The  $G\alpha_{i/z}$  pathway is mainly responsible for PAR1's inhibition of adenylyl cyclase (AC). AC catalyzes the conversion of ATP to cAMP and the inhibition of this conversion lowers cAMP levels and causes a corresponding decrease in protein kinase A (PKA) activation [9]. This cascade serves to modulate Raf activation via Ras activation. Raf then relieves the inhibition of AC shutting down the cascade [14]. The  $\beta\gamma$  subunits, *per se*, may play a role in the transcriptional response and cell mobility through effectors such as PI3-kinase, PLC $\beta$ , K<sup>+</sup> channels, and G-protein coupled and non-receptor tyrosine kinases. However, particularly in platelets, the function of the  $\beta\gamma$  subunits is less well-established [30].

Finally, PAR1 has also been shown to signal through a 33 kDa serine-threonine protein kinase (PK33) in platelets. PK33 is activated within seconds of either thrombin or PAR1-AP addition to platelets, and may be linked to potentiating the aggregation [32] which is induced by the PLC $\beta$  pathway.

Therefore, activated PAR1 couples with several signalling cascades which are interrelated and interdependent, and coordination of the receptor's activity relies heavily on switch kinases which provide relay stations for the integration of intracellular signals.

### **1.3.2 Focus on Ca<sup>2+</sup> mobilisation and store-operated Ca<sup>2+</sup> entry (SOCE)**

The present study assessed the signalling mechanism related to the mobilization of Ca<sup>2+</sup> in response to PAR1-AP in PAR1-Sf9 cells using pharmacological tools in an attempt to dissect out its various components.

In a GPCR signalling system,  $G\alpha_q$  has been associated with the mobilisation of  $Ca^{2+}$ . As previously mentioned, the PAR1- $G\alpha_q$  interaction leads to the activation of PLC $\beta$ . Activation of PLC $\beta$ , which can be inhibited by using D609, mediates the hydrolysis of phosphatidylinositol 4,5-bisphosphate (PIP<sub>2</sub>) and subsequent formation of IP<sub>3</sub> and DAG. Newly formed IP<sub>3</sub> binds to IP<sub>3</sub> receptor (IP<sub>3</sub>R)-  $Ca^{2+}$  channels, located in the membrane of the endoplasmic reticulum (ER), and activates an efflux of  $Ca^{2+}$  from the ER into the cytosolic space [33]. These  $Ca^{2+}$  channels are importantly regulated by the presence of IP<sub>3</sub> and  $Ca^{2+}$  sensors located directly on the channel as well as by a number of protein kinases including PKA and PKC [33]. IP<sub>3</sub>R-  $Ca^{2+}$  channels can be inhibited either specifically through the use of TMB-8 [34] or concurrently with plasma membrane  $Ca^{2+}$  channels by using D-600 [35].

The intracellular  $Ca^{2+}$  concentration ( $[Ca^{2+}]_i$ ) is regulated by a plasma membrane  $Ca^{2+}$  pump mediated transport which extrudes  $Ca^{2+}$  from the cytosolic space out of the cell which is energized by adenosine triphosphate and by a thapsigargin-sensitive  $Ca^{2+}$ -ATPase which transports cytosolic calcium into the ER and other organelles [36].

Inhibition of the activity of PKA through the use of H-89 [37] would remove its contribution to modulating the IP<sub>3</sub>R-  $Ca^{2+}$  channel activation.

The depletion of  $Ca^{2+}$  from the ER is detected by stromal interacting molecule-1 (STIM-1) [38]. The activation of STIM-1 allows for its translocation to puncta, which refers to the interface between the ER and the plasma membrane. Once translocated to puncta, STIM-1 activates Orai-1 channels [39]. Orai-1 channels belong to a novel class of  $Ca^{2+}$  channels which may function as L-type  $Ca^{2+}$  channels and are lanthanum ion ( $La^{3+}$ )-sensitive [38, 39].

The entry of  $\text{Ca}^{2+}$  from the extracellular space can be controlled either by using a  $\text{Ca}^{2+}$ -free medium or by inhibiting  $\text{Ca}^{2+}$  entry with  $\text{Ca}^{2+}$  channels inhibitors, such as  $\text{La}^{3+}$  [40], nifedipine [35] or D-600 [35].

The second by-product of PIP<sub>2</sub> hydrolysis is DAG. DAG is a principal activator of PKC within cells. PKC, so named as it is a  $\text{Ca}^{2+}$ -sensitive protein kinase, is a key modulator in the mobilization of  $\text{Ca}^{2+}$  throughout the cell. PKC activity is associated with  $\text{Ca}^{2+}$  channel phosphorylation and inactivation, including the inactivation of Orai-1 channel phosphorylation [41]. It may also play a role in the phosphorylation of IP<sub>3</sub>R-activated  $\text{Ca}^{2+}$  channels [33, 42].

The inhibition of PKC with bisindolylmaleimide [43] would prolong any increase in  $[\text{Ca}^{2+}]_i$  while the use of PDBu would potentiate PKC activity [44, 45], hastening the phosphorylation of PKC targets, including  $\text{Ca}^{2+}$  channel phosphorylation and inactivation.

### **1.3.3 Inactivation of the receptor**

PAR1 inactivation is a two-step process. Initially, phosphorylation of serines and threonines on the cytoplasmic C-tail occurs, and is attributed to at least two protein kinases. The first is a PKC, and the second is a presumed G-protein receptor specific kinase, the beta-adrenergic receptor kinase-2 ( $\beta$ ARK2) [45]. Approximately 85% of the cell surface receptors are internalized in coated pits within one minute of activation; most of these are targeted to lysosomes [46]. Receptor internalization is specific to activated PAR1 [47] and the rate of reappearance of the cell's response to thrombin suggests that *de novo* synthesis of the receptor is required. However, recovery from the desensitized state, in response to PAR1-AP addition, can occur in mammalian cells within 30 to 60 minutes [47], suggesting some receptor recycling to the cell membrane.

In endothelial cells and fibroblasts, a population of PAR1s located in intracellular pools has been identified [48]. These are transported to the cell surface following thrombin stimulation, allowing the cell to be reactivated rapidly. In platelets, it is unlikely that reappearance of receptors at the surface is required since platelets are activated only once [8].

#### **1.3.4 Recent advances in understanding PARs**

Numerous biochemical advances have been made since the initial discovery of PAR1. To begin with, other proteases have recently been shown to cleave and activate PAR1, including factor Xa [49], plasmin [50], kallikreins [51, 52], activated protein C (APC) [53], matrix metalloproteinase-1 (MMP1) [54], neutrophil elastase (NE) [55] and neutrophil proteinase-3 (PR3) [55]. The cleavage by these proteases reveals receptor-activating sequences that differ from each other [55] and are classified as ‘non-canonical’ tethered ligands. Synthetic peptides derived from this ‘non-canonical’ cleavage of PAR1 (e.g. TLDPRSF-NH<sub>2</sub> for a PR3 tethered ligand derived-activating peptide, or RNPNDKYEPF-NH<sub>2</sub> for a NE tethered ligand-derived activating peptide) can serve as ‘biased’ agonists of PAR1 to activate selective components of signalling, like MAPK, but not calcium signalling [55].

At present, PAR signalling is known to activate several major signal pathways. First, and that which is the focus of this study, is the ‘classical pathway’ in which receptor activation causes signalling via G-proteins and downstream targets.

It is, however, important to note that two additional pathways have been associated with PAR1 activity. The first of these includes a beta-arrestin signalling pathway involving ligand-regulated scaffolds [56]. Arrestin-bound GPCRs are uncoupled from their classical G-

proteins to activate other signalling pathways [57]. Arrestin-dependent signals can be initiated by ‘biased’ agonists, creating the potential for drugs that can modulate specific GPCR function.

It has recently been discovered that PARs are able to function both as monomeric receptors and as partners in a variety of complexes including homo- and heterodimers consisting of PAR-PAR, PAR-GPCR and PAR-non-GPCR [58]. This transactivation of a variety of receptors [58] and other signalling constituents (e.g. ion channels) is thought to occur through specific signalling components rather than by a physical interaction.

The advances in the understanding of PARs point to the importance of studying the components of the PAR1  $Ca^{2+}$  signalling cascade in that it could be critical to regulating one or more of the actions of the receptor.

#### **1.4 *Spodoptera frugiperda* (Sf9) cell line**

Sf9 cells originate in the ovary of the fall armyworm *Spodoptera frugiperda*. These cells are susceptible to infection by baculovirus type viruses. The baculovirus expression system is widely used for heterologous expression since it provides a eukaryotic environment which is ideal for the production of viable proteins, including mammalian proteins. The use of recombinant baculovirus has previously been used as a high-output expression system for mammalian proteins, including cell-surface receptors [59]. The baculovirus expression system functions in a simple viral fashion. Infectious particles enter the host cells by receptor-mediated endocytosis [60] and the viral DNA is uncoated in the nucleus. Within 6 hours the entire viral DNA begins to replicate, at first releasing viral particles into the extracellular environment (also known as the budded virus). The budded virus is responsible for the

infection in cell culture [60]. The later phase of infection is characterized by the appearance of occluded virus particles embedded in a polyhedrin protein.

This polyhedrin protein is maximally expressed in the late phase of infection. However, this phase is not necessary for the viability of the virus in cell culture. Insertion of heterologous DNA in place of the polyhedrin allow for replication to be controlled by the polyhedrin promoter, thus producing recombinant baculovirus in large quantity. Infection of Sf9 cells according to this method allowed us to express a rat PAR1 which was believed to have proper folding, disulfide bonds, oligomerization, and most post-translational modifications.

It is believed that the pharmacology of GPCR expressed using the Sf9/baculovirus system is similar to that in mammalian systems [40].

It is well known that Sf9 cells possess an intrinsic seven transmembrane, GPCR for octopamine, a neurotransmitter. Functional studies have established that activation of this receptor and coupling to  $G\alpha_s$  yields an increase in intracellular calcium through the release of  $Ca^{2+}$  from intracellular stores [61]. The Sf9 cell membrane is equipped with a potassium ( $K^+$ )/hydrogen ( $H^+$ ) ion exchanger, a chloride ( $Cl^-$ ) channel, a muscarinic (M3)-G-protein coupled  $K^+$  channel and two distinct  $Ca^{2+}$  channels, one which is activated secondary to intracellular  $Ca^{2+}$  release from intracellular pools and is sensitive to lanthanum ions ( $La^{3+}$ ), and one which is muscarinic (M5) and is barium, gadolinium, and  $La^{3+}$ -sensitive [40, 62].

The existence of several G-protein forms have been identified in Sf9 cells. These include  $G\alpha_{i/z}$ ,  $G\alpha_{12/13}$ ,  $G\alpha_s$  and  $G\alpha_q$  [26]. Both  $G\alpha_{i/z}$ ,  $G\alpha_{12/13}$  are found at lower levels while higher levels of  $G\alpha_s$  and  $G\alpha_q$  have been identified [63].



It is believed that the insect cell  $G\alpha_{i/z}$ -like proteins do not couple to mammalian GPCR whereas the remaining forms have been shown to couple to various mammalian receptors [40].

A number of additional signal transduction components have been identified in Sf9 cells, including the presence of AC, PLC, and GPCR kinase [40].

Therefore, expression of rPAR1 in Sf9 cells was meant to take advantage of a system made up of an isolated exogenous mammalian receptor coupled to the insect cell endogenous signalling cascades, especially that of intracellular calcium signalling, for the study of its activation by PAR1-AP, using Fura-2 microspectrofluoroscopy.

### **1.5 Rationale, hypothesis and objectives**

The **rationale** of the current study was largely based on the material exposed in the previous sections. The important points that justify the present work are summarised below:

1. The Sf9 insect cell system is an excellent way to express membrane proteins in large amount and at low cost;
2. Sf9 cells have been shown to possess several components of the calcium signalling cascade, including  $G\alpha_{i/z}$ ,  $G\alpha_{12/13}$ ,  $G\alpha_s$  and  $G\alpha_q$ , several of them being also found in mammalian cells;
3. Calcium signalling is one of the several signalling mechanisms triggered by PAR1 activation in mammalian cells (Figure 5). The exact mechanisms involved in the calcium response to PAR1 activation remain largely unknown, but are believed to represent new therapeutic targets for PAR-related pathologies.

It was therefore **hypothesized** that:

1. the Sf9-baculovirus system represents a valid receptor expression tool for rPAR1, a mammalian GPCR, in isolation from other mammalian receptors;
2. this exogenous protein functionally couples to the intrinsic Ca<sup>2+</sup> signalling apparatus of Sf9 cells.

Consequently, the **objectives** of the study, and the associated **approaches** were:

1. to determine whether rPAR1 is expressed and localized on the Sf9 cell surface, using immunofluorescence, confocal microscopy and fluorescence-activated cell sorting (FACS);
2. to demonstrate that the receptor is coupled to Sf9 cells' calcium signalling, using single cell Fura-2 microspectrofluoroscropy;
3. to identify components of Sf9 cells' calcium signalling machinery involved in mammalian rPAR1 activation, using pharmacological modulators that inhibit calcium transport in the plasma membrane channels (D-600, nifedipine, lanthanum), calcium sequestration in intracellular stores (thapsigargin) and calcium efflux from intracellular stores (TMB-8), and that modulate the functions of PLC $\beta$  (D-609, an inhibitor), PKA (H-89, an inhibitor) and PKC (PDBu, an activator; bisindolylmaleimide, an inhibitor).

## **MATERIALS AND METHODS**

## 2.1 Construction of the recombinant baculovirus rPAR1 and virus preparation

Construction of the rat PAR1 recombinant baculovirus was prepared using the Blu-Bac (Invitrogen, Life Technologies, Burlington, ON) system for viral production. Messenger ribonucleic acid (mRNA) was purified from male Sprague Dawley rat lung tissue and transformed into single stranded complementary deoxyribonucleic acid (cDNA) by reverse transcriptase-polymerase chain reaction (RT-PCR) using oligo (dT) primers and Moloney murine leukemia virus reverse transcriptase. Primers for nested PCR were designed according to the published sequence of the rPAR1 [64]. The primers: 5'threc-TTGGATCCACAATGGGGCCCCGGCGCT-3' (bp 71-89) and 5'threc-TTCCAAGGTA CTTCTTTTCCCATGGCC-3' (bp 1315-1334), used for second round PCR incorporated BamHI and KpnI restriction sites at the 5' and 3' ends of the amplified product. Purified bacmid PCR II containing the rat PAR1 sequence obtained after transformation into *E.coli* MC1061 was sequenced and subcloned into the baculovirus transfer vector pJVETL at the BamHI/KpnI sites. Cotransfection into Sf9 cells with linearized *Autographa californica* nuclear polyhedrosis virus (AcMNPV) using the lipofectin reagent yielded the recombinant virus.

The recombinant virus was plaque purified through three rounds and blue plaques were selected in the presence of 5-bromo-4-chloro-3-indolyl-beta-D-galacto-pyranoside (X-Gal) and tested for the presence of occlusion virus. At each stage of plaque purification, the presence of receptor cDNA was confirmed by dot-blot analysis of infected cell lysates hybridized to a 784bp cDNA probe. Virus stocks were amplified, at 22°C, in Sf9 cells by infection of 40ml of cells at  $1 \times 10^6$  cells/ml for 72 hours and collected.

## **2.2 Infection procedure**

The Sf9 cells were grown in shaked capped Erlenmeyer flasks (Corning, Montreal, QC) at room temperature (22°C). The growth medium, Grace's Simplified Eagle's Medium (Gibco BRL Life Technologies, Burlington, ON), was supplemented with 10% heat-inactivated fetal bovine serum (FBS) (Hyclone, ThermoScientific, Menomonee Falls, WI, USA), and 0.1% pluronic acid F-68.

The cells were grown between passages 6 and 65. Immediately after each passage, densities ranged from 2 to  $6 \times 10^5$  cells/ml. They were then grown to densities between 1.5 and  $3 \times 10^6$  cells/ml. Cell seeding for infection was performed by allowing cells to attach to the bottom of capped plastic culture flasks and further grown to cell counts in the range of 3 to  $8 \times 10^5$  cells/ml with virus addition performed at a multiplicity of infection (MOI) of 15.

rPAR1-Sf9 cells were used for experiments between 25-48 hours following virus infection, and all assays were conducted at room temperature (22°C).

## **2.3 Detection of expressed receptor in cell membranes**

### **2.3.1 Receptor-antibody cross-linking studies in rPAR1-Sf9 cells**

The binding assay was performed in essentially the same manner as the cross-linking assay, although the latter required the addition of a cross-linker. Cells were prepared by growing to confluency in 6 well plates and rinsed three times with a refrigerated 0.1% bovine serum albumin (BSA)/ phosphate buffered solution (PBS), each rinsing occurring at 10 minute intervals with intermittent refrigeration. In individual centrifuge tubes, 500µl of solution containing the desired concentration of ligand diluted with 0.1% BSA/PBS was added, along with rPAR1 expressing cells, and incubated on ice for three hours. The tubes were labelled in the following manner: tube 1, 30nM hot; tube 2, 200nM hot; tube 3, 1000nM hot: tube 4, 30nM hot + 6µM

cold; tube 5, 200nM hot + 40 $\mu$ M cold; and tube 6, 1000nM hot + 200 $\mu$ M cold (where: 'hot' refers to iodine labelled PAR1-AP while 'cold' refers to the non-iodinated PAR1-AP) The ligand was then aspirated and the cells washed once with ice cold PBS. In the cross-linking experiment the cross-linker was added by the addition of 5mM bis (sulfosuccinimidyl) suberate (BS3) in PBS, followed by incubation and refrigeration for 5 minutes, addition of 100mM glycine, another 5 minute incubation, and rinsing twice with 2ml PBS. In all assays cell lysis was important, and was performed by the addition of a modified PBS solution made up of 1% triton X-100, 1mM ethylene-glycotetraacetic acid (EGTA) (Caledon Labs, Georgetown, Ontario, Canada), 1mM phenyl methyl sulfonyl fluoride, 10 $\mu$ g/ml pepstatin (Sigma-Aldrich Chemicals, Milwaukee, WI, USA), 10 $\mu$ g/ml leupeptin, 10 $\mu$ g/ml antipain, 10 $\mu$ g/ml benzamidine hydrochloride (HCl), 10 $\mu$ g/ml soybean trypsin inhibitor, 10 $\mu$ g/ml aprotinin.

After centrifugation for 10 minutes at 13000 revolutions per minute (rpm) and 4°C, the supernatant containing the receptor was retrieved and placed in a gamma-counter prior to resolution on a 3-15% linear gradient sodium dodecyl sulfate polyacrylamide gel electrophoresis (SDS-PAGE) and autoradiographed.

### **2.3.2 Western blot membrane preparation and endoglycosidase treatment of rPAR1**

Crude membranes were obtained according to the method previously described by Vouret-Craviari & al, 1995 [65] with slight modifications. Sf9 cells in culture were infected with baculovirus rPAR1 at an MOI of 15, grown for 48 hours and collected at 500 x g. Cells were rinsed twice with 10mM tris (hydroxymethyl) aminomethane (Tris), pH 7.5, 1mM EGTA before harvesting in tris (hydroxymethyl) aminomethane buffer (TB) (5mM Tris, pH 7.5) 0.5mM EDTA; 10 $\mu$ g/ml each of the protease inhibitors leupeptin, aprotinin, pepstatin,

1mM Pefabloc<sup>R</sup> and phosphatase inhibitors 1mM orthovanadate and 50mM sodium fluoride (NaF) and incubated on ice for 5 minutes. Subsequently, cells were disrupted by sonification and nuclei were removed by centrifugation (2000 rpm for 10 minutes at 4°C). After centrifugation, crude membranes were resuspended in the same buffer and treated with endoglycosidase F according to the New England Biolabs' (Ipswich, MA) protocol, except that all indicated procedures were carried out at room temperature. Treated membranes were then applied onto a 7.5 % electrophoretic gel left running at 50 volts (V) for 2 hours. The separation gel was prepared for immunoblot with a solution comprised of 60ml methanol, 3ml 0.1% SDS, 909mg tris and 4.3mg glycine in a total volume of 300ml water (H<sub>2</sub>O).

Samples were separated on sodium dodecyl sulphate-polyacrylamide gel electrophoresis (SDS-PAGE) and blotted onto Hybond-C nitrocellulose membranes. The membranes were blocked with 0.5% I-Block (Applied Biosystems distributed by Life Technologies, Burlington, ON) and 0.3% Triton X-100 (Sigma-Aldrich Chemicals, Milwaukee, WI, USA) in PBS at 4°C and incubated for 1 hour (h) with specific antibodies (supplied by Dr. M.D. Hollenberg of the University of Calgary, Department of Medicine): anti-rPAR1 antibody (1:500 dilution), anti-mPAR2 antibody (1:500 dilution) or pre-immune serum (1:500 dilution). After a 30 minute wash, the membranes were incubated with anti-rabbit horseradish peroxidase-linked secondary antibody for 1h and washed for another 30 minutes. Immunoreactive protein signals were detected using the chemiluminescence (ECL) detection system from Amersham (distributed by GE Life Sciences, Baie d'Urfé, QC).

### **2.3.3 Immunocytochemistry, fluorescence-activated cell sorting (FACS) and confocal microscopy**

FACS allows for a quantitative analysis using cell sorting and laser-activated detection in a flow cytometer system whereby a suspension of cells is held in a funnel-like chamber. The system uses hydrodynamic focusing of the suspended cells (cell sorting), around a light source typically found in the narrower portion of the chamber. The addition of a fluorescent probe (Oregon green-tagged polyclonal antibodies) to the cell suspension mixture increases the amount of fluorescence measured by the detection system located in close proximity to the light source, the scattered light, and any background fluorescent light. The fluorescence intensity is plotted as a function of cell number.

Confocal microscopy is a high resolution imaging technique in which the excitation of a fluorophore (in our experiments, Oregon-green tagged polyclonal antibodies) is ensured through laser excitation of the sample, using a xenon lamp. A confocal microscope uses the illumination of a single point of the sample and a pinhole in the emitted light pathway to measure the intensity of emitted light from a restricted field and in a narrow-thickness of sample slices. Only the light in a given spatial plane is detected at a given time within a corresponding confocal slice of about 0.2 to 0.3 $\mu$ m in width. Individual images of slices are obtained by scanning the sample line by line and three dimensional images are reconstructed using sequential vertical slices of the sample.

Sf9 cells infected with rPAR1-cDNA were grown for 48h using the techniques described above. Cells in suspension FACS or plated on glass coverslips (for confocal microscopy) were washed twice with PBS (three times for confocal microscopy) and fixed with fresh 3% (v/v) formaldehyde in PBS for 20 minutes. Non-specific binding sites were blocked with PBS containing 1% I-Block (PBS-I-Block) for 1h at room temperature. The cells



were then incubated for 1h at room temperature with anti-rPAR1 receptor antibodies or pre-immune serum diluted 1:50 in 0.5% PBS-I-Block. After three washings with 0.5% PBS-I-Block, cells were incubated with Oregon-green-conjugated anti-rabbit immunoglobulin (Ig) G (1:2000 dilution, 1h at room temperature), used to reveal the primary antibodies. The cells were detected using a Beckman-Coulter XL-MCL flow cytometry system (Mississauga, ON).

For confocal microscopy, rPAR1-Sf9 cells were left to adhere to 24mm circular glass coverslips for 30 minutes using the same method as that described for microspectrofluorescence. Cell surface receptors were detected by Molecular Dynamics CLSM 2001 confocal microscope with inverted Nikon Diaphot fluorescent microscope (Amersham Biosciences, Sunnyvale, CA, USA) using techniques previously described [66-68].

## **2.4 Functional assays**

### **2.4.1 Solutions**

Measurements of calcium transients were conducted in one of three experimental media: 2.8 Grace simplified medium (GSM), 6.8GSM, or 0GSM. The media were composed of either 2.8mM or 6.8mM  $\text{CaCl}_2$ , 2  $\text{H}_2\text{O}$  or 2mM EGTA, 54.6mM KCl, 11.4mM  $\text{MgCl}_2 \times 6 \text{H}_2\text{O}$ , 11.3mM  $\text{MgSO}_4 \times 7 \text{H}_2\text{O}$ , 11.2mM NaCl, 7.14mM PIPES- dipotassium salt, 2.86mM PIPES-acid, 3.9mM D-glucose and adjusted to 340-380mOsm with sucrose, and a pH=6.4 with KOH.

All peptidomimetic compounds were prepared in distilled and deionized  $\text{H}_2\text{O}$  to a stock concentration of 5mM and subsequently diluted to a final volume of 500 $\mu\text{l}$  in the experimental solution.

#### 2.4.2 Preparation and use of agonists and signal modulators

Octopamine was used as a 5mM stock solution in H<sub>2</sub>O. Experiments were conducted using 20µl of stock solution in 480µl of 2.8 or 0GSM.

Aliquots of thrombin were prepared using thrombin from human plasma (Sigma-Aldrich Chemicals, Milwaukee, WI, USA) diluted in H<sub>2</sub>O to produce a stock solution of 250U/ml. Experiments were also conducted using 20µl of stock solution with 480µl of 2.8 or 0GSM.

PAR1-AP was provided by the Peptide Synthesis Facility at BioChem Therapeutics (Laval, Quebec) as lyophilized powder. A 2mM stock solution was prepared using 20% EtOH / 20% DMSO / 60% H<sub>2</sub>O. Experiments were conducted using 50µl of stock solution in 450µl of 2.8 or 0GSM, to a final, supra-maximal dose of 100µM.

A solution of 5mM La<sup>3+</sup> was prepared using 50ml H<sub>2</sub>O and 1.021g LaCl<sub>3</sub> (Calbiochem, La Jolla, CA, USA) to produce a stock solution of 55mM. Experiments were conducted using 50µl LaCl<sub>3</sub> solution in 500µl of 2.8GSM.

Stock solutions for 3,4,5-trimethoxybenzoic acid 8-(diethylamino)octyl ester (TMB-8) (Alomone Labs, Jerusalem, Israel) as well as N-[2-[[3-(4-bromophenyl)-2-propenyl]amino]ethyl]-5-1 isoquinolinesulfonamide (H-89) (Sigma-Aldrich Chemicals, Milwaukee, WI, USA) and were prepared using H<sub>2</sub>O and tricyclodecan-9-yl xanthogenate (D-609) (Alomone Labs, Jerusalem, Israel),phorbol 12,13 dibutyrate (PDBu) (Sigma-Aldrich Chemicals, Milwaukee, WI, USA) and bisindolylmaleimide (Sigma-Aldrich Chemicals, Milwaukee, WI, USA) were prepared using DMSO (Sigma-Aldrich Chemicals, Milwaukee, WI, USA) in a manner similar to La<sup>3+</sup>.

Nifedipine (Calbiochem, La Jolla, CA, USA) and methoxyverapamil (D-600) (Calbiochem, La Jolla, CA, USA) were diluted in DMSO to obtain stock solutions of 0.5mM and 5mM, respectively. Serial dilution of 20µl of stock solution in 230µl of GSM was performed and subsequently added to the experimental chamber which contained a starting volume of 250µl, for a total final volume of 500µl.

A stock solution of 50µM thapsigargin (Alomone Labs, Jerusalem, Israel), was also prepared using DMSO, and cells were bathed with 50µM thapsigargin in 500µl 0GSM for 5 minutes prior to the addition of 100µM PAR1-AP.

### **2.4.3 Microspectrofluorescence**

Functional coupling of rPAR1 in the rPAR1-Sf9 cells was studied using a Photon Technology International's DeltaRam/microscope (PTI) photometer system. A xenon lamp was used as a light source, and emitting light at alternating wavelengths of 340 and 380 nanometres (nm), directed via a 40x epifluorescence objective, at the Sf9 cells plated on coverslips and loaded with Fura-2 (Molecular Probes, Eugene, Oregon). The fluorescent probe Fura-2 fluoresces in response to this excitation, with the amount of light being a function of the  $[Ca^{2+}]_i$ . The emitted fluorescence is captured through a 505nm emission filter by a photon-counting detector connected to a computer.

Fura-2 cell loading was realized by using the Fura-2 AM fluorophore (Molecular Probes, Eugene, Oregon), a cell permeant compound. Fura-2 AM is hydrolyzed by intracellular esterases to form Fura-2 which remains trapped in the cells. Upon binding to  $Ca^{2+}$ , the excitation spectra of Fura-2 undergoes a shift in fluorescence to lower wavelength. This spectral property of Fura-2 was used for high-sensitivity determination of intracellular  $Ca^{2+}$  concentration. Using the ratio

of Fura-2 intensities from cells excited at 340nm and 380nm provides higher dynamic range and makes the measurements largely independent of volume change artefacts. Therefore, fluorescence ratio versus time was used to determine the cellular response in the functional assays. The procedure to obtain intracellular calcium concentration from fluorescence intensities and ratios is described in Appendix 1.

Between 25 and 48 hours post infection, 500  $\mu$ l of cells were plated onto 24mm circular glass slides and left to adhere for 30 minutes. Once attached, the cells were rinsed twice with 6.8GSM. Cells were then loaded with the  $\text{Ca}^{2+}$ -insensitive Fura-2 AM and washed three times following 30 minutes of incubation at room temperature.

Fura-2 measurements were performed on single cells that were optically isolated under microscopic observation by means of an adjustable rectangular aperture located in the emission path of the microspectrofluorometer.

Results are presented as normalized ratio, with baseline  $[\text{Ca}^{2+}]_i$  levels adjusted to ratio level 1, for simplicity sake. Fluorescence ratios were normalized according to the following transformation:

$$(F340/F380)/(F340/F380)_{t=0}$$

Glass coverslips were then mounted in a custom-made experimental chamber containing a final volume of 1ml of 2.8GSM or 0GSM.

All figures are representative of at least 3 identical experiments.

# **RESULTS**

### **3.1 Sf9-baculovirus expression system of rPAR1 receptor**

#### **3.1.1 Successful expression of rPAR1**

In order to establish the successful expression of rPAR1 using the Sf9-baculovirus expression system, assays were initially conducted as described in the Materials and Methods (section 2.3).

To evaluate protein expression of rPAR1 in rPAR1-cDNA-containing baculovirus infected Sf9 cells (rPAR1-Sf9), western blots were performed as shown in Figure 6. Western blot analysis uses gel electrophoresis to separate proteins by molecular weight. Smaller proteins migrate more quickly through the polyacrylamide gel while larger proteins migrate more slowly. The anti-PAR1 antibody recognized a band in membranes obtained from Sf9 insect cells infected with ratPAR1-cDNA containing baculovirus, as shown in Figure 6, lane 5. The band seen with the anti-rPAR1 antibody was specific to rPAR1 since it was absent in the non-infected Sf9 cells (lane 4) and the pre-immune serum (lanes 1-3).

Given that potential sites for N-linked glycosylations are present on rPAR1, freshly prepared membranes from rPAR1-Sf9 or Sf9 wild type were treated with N-glycosidase F to remove all asparagine-linked carbohydrates from the protein. The deglycosylation resulted in a decrease in the apparent molecular mass for rPAR1 to approximately 40kDa. This is consistent with the literature which indicates that while the mature receptor has a molecular mass ranging from 68 to 80 kDa, N-linked glycosylations represent 32-40 kDa [65].

Anti-rPAR1 antibodies (supplied by Dr. M.D. Hollenberg of the University of Calgary, Department of Medicine) were used to perform western blot analysis.

Binding and cross-linking studies were attempted using radioiodinated peptides in order to confirm the binding specificity of the PAR1-AP. A total of three attempts failed to be

successful, and it was later discovered that the antibody iodination process had been unsuccessful and further cross-linking studies were not attempted. However, various other assays were used to determine successful receptor expression.

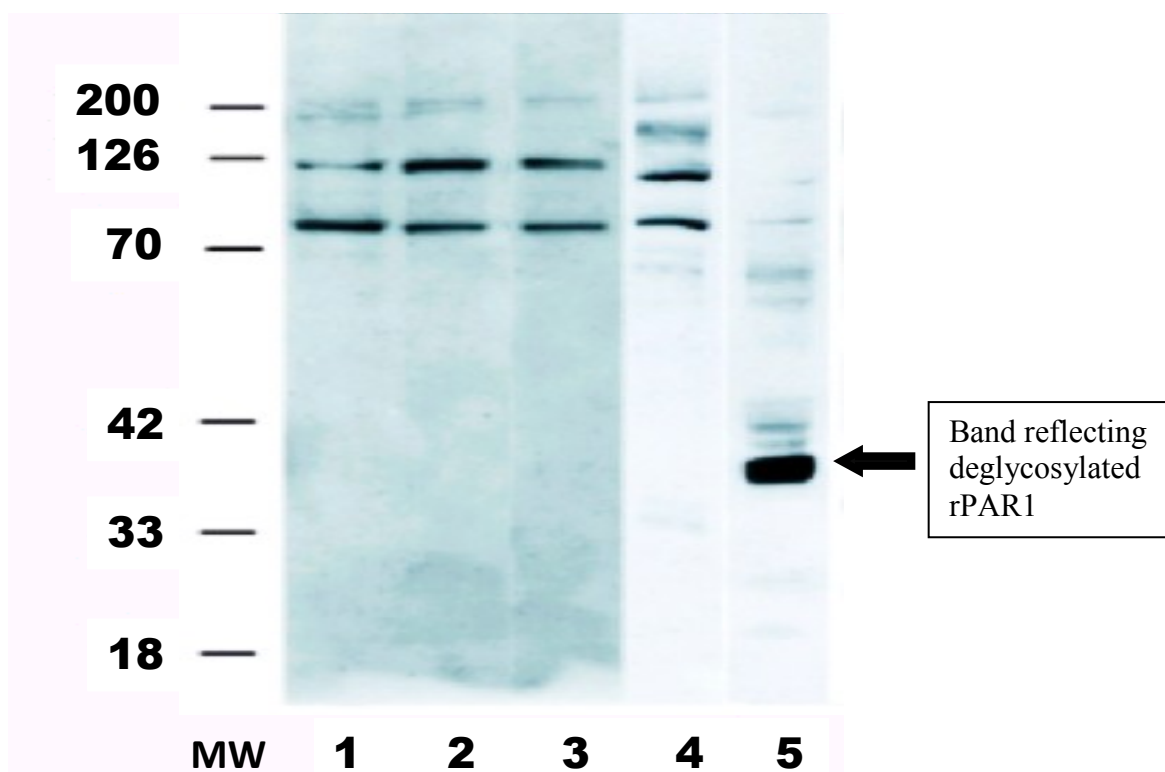


**Figure 6: Western blot analysis of rPAR1 infected Sf9 cells.** MW: molecular weight markers (kDa). **Lanes 1-3:** pre-immune serum in non-infected Sf9 (lane 1), rPAR1 infected Sf9 (lane 2), and mPAR2 infected Sf9 (lane 3). **Lanes 4 and 5:** anti-rPAR1 antibody: non-infected Sf9 cells (lane 4), rPAR1 infected Sf9 cells (lane 5).

### 3.1.2 Localization of the rPAR1 receptor expressed in Sf9 cells

#### 3.1.2.1 Receptor localization using FACS

Assays were performed using immunocytochemistry techniques to determine whether translocation of the protein to the cell surface had been successful. The first of these were conducted using FACS. Results are shown in Figure 7. The baseline level of scattering and

emission of light by the rPAR1 infected Sf9 cells is shown in green (control). This control contains neither preimmune serum nor tagged-antibody. The blue line depicts the fluorescence measured in rPAR1-Sf9 cells which have been treated with preimmune serum (serum-control). Results are virtually superimposed, with fluorescence being only slightly affected by the incubation with pre-immune serum, which may mainly be due to autofluorescence of serum proteins. As shown by the red curve, the rPAR1-Sf9 cells treated with anti-rPAR1 tagged antibodies emitted a higher level of intensity due to the cell-surface linked fluorescent probes, demonstrating the successful expression of the rPAR1 on the cell plasma membranes of infected Sf9 cells (Figure 7).

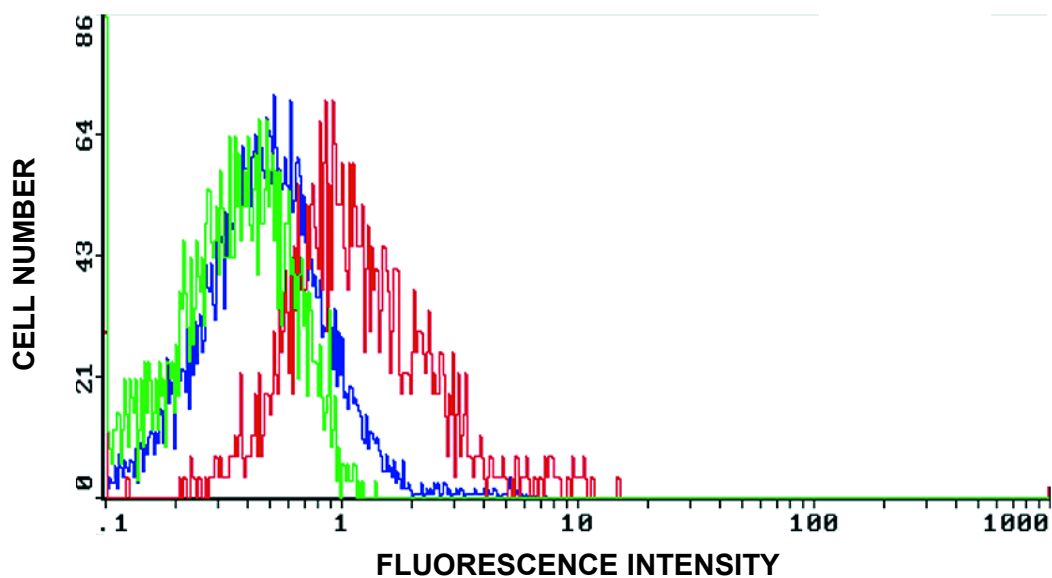


**Figure 7: FACS analysis of rPAR1 expression** Green curve: non-infected Sf9 cells with no preimmune serum and without tagged antibodies. Blue curve: rPAR1-infected Sf9 cells with preimmune serum. Red curve: rPAR1-infected Sf9 cells with anti-rPAR1-antibody. The shift to the right of the curve indicates linking of fluorescent-tagged secondary antibodies. Samples were made of 100 cells each.

### 3.1.2.2 Receptor localization using confocal microscopy

Confocal microscopy was also used to establish successful rPAR1 expression and to find out where the receptor was localized. As shown in Figure 8, confocal images using



Oregon-green tagged polyclonal antibodies demonstrated that the rPAR1 receptors were expressed and translocated mainly onto the surface of rPAR1-Sf9 cells (Figure 8 images 4 and 6). The results showed also that some receptors were located in the cytoplasmic space (Figure 8 images 2, 3 and 5), representing either a mature or a functional receptor pool, or both, or were simply reflective of receptor cycling.

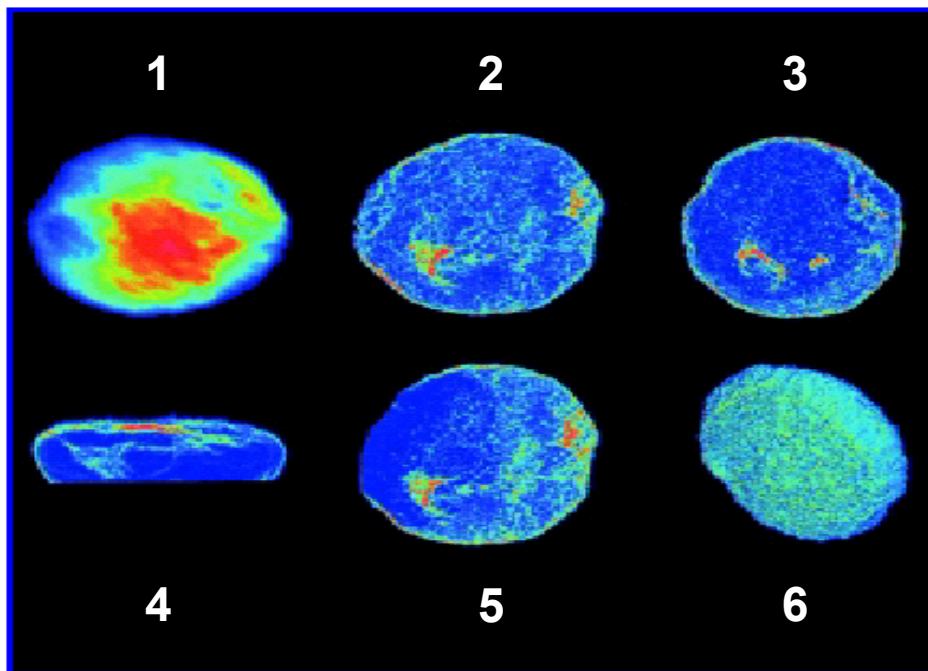


**Figure 8: Different views of confocal micrographs of a single Sf9 cell expressing rPAR1.** 1: top view of the cell. 2, 3 and 5: view of individual cell slices showing fluorescent receptors concentrated along the periphery of the cell as well as areas of increased receptor density in the cytoplasmic space (in green) . 4: vertical view of the cell, clearly demonstrating the location of the rPAR1 along the cell surface. 6: bottom surface of the cell (closest to the glass coverslip) showing dense localization of the fluorescent receptors on the cell surface.

### 3.2 Changes in $[Ca^{2+}]_i$ concentration using octopamine

Control experiments were conducted to establish that  $[Ca^{2+}]_i$  changes could be observed in wild-type and infected Sf9 cells in response to the endogenous agonist octopamine [69]. Wild-type Sf9 cells are known to respond to octopamine as the activation of

the cell-surface receptors yields intracellular  $\text{Ca}^{2+}$  signals detected using Fura-2 [70].

Therefore, the octopamine test was used to ensure the physiological competence of wild-type and baculovirus-infected Sf9 cells used in the present work.

Figure 9 (green trace) shows the  $[\text{Ca}^{2+}]_i$  of a single wild-type Sf9 cell following the addition of 100  $\mu\text{M}$  octopamine in the absence of external calcium (0GSM). As expected, 100  $\mu\text{M}$  octopamine induced a surge in  $[\text{Ca}^{2+}]_i$ . In the calcium-containing experimental medium (2.8GSM), the initial  $[\text{Ca}^{2+}]_i$  surge was followed by a second phase consisting of a longer-lasting plateau (Figure 9, violet trace). Initial studies suggested that the octopamine response may point to an influx of  $\text{Ca}^{2+}$  [70], and subsequent studies supported the findings that this second phase of the octopamine response was likely a calcium influx through  $\text{Ca}^{2+}$  channels of the cell membrane [69].

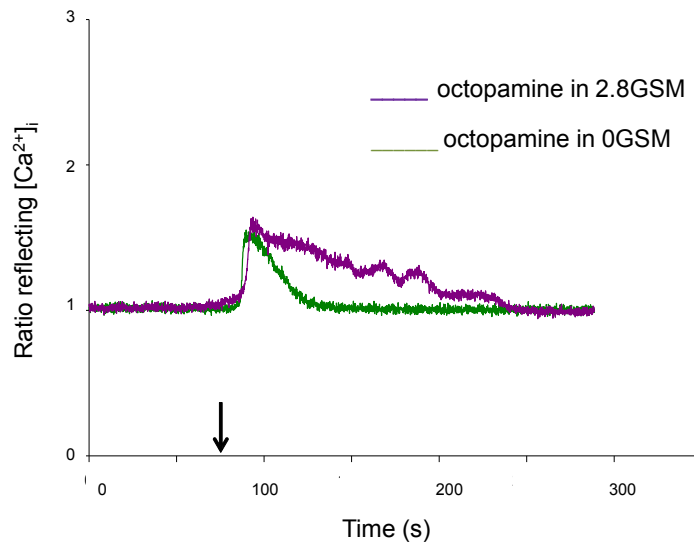


**Figure 9: Effect of octopamine on cytosolic calcium in wild-type Sf9 cells.**

Sf9 cells were stimulated by the addition of 100  $\mu\text{M}$  octopamine (as indicated by the arrow) in the presence of extracellular  $\text{Ca}^{2+}$  (violet trace) or in the absence of extracellular  $\text{Ca}^{2+}$  (green trace). Data reported is representative of three identical experiments.

The octopamine test was used in infected cells to determine whether the pathogen would ultimately affect the Sf9's functionality and to determine the optimal time window to be used for the functional assays of rPAR1 expressed in the cells. Although biphasic responses were generally recorded, a significantly reduced competency of the cells was observed after prolonged viral exposure (Figure 10). These experiments demonstrated also that the octopamine receptors remained functional in rPAR1 expressing cells.

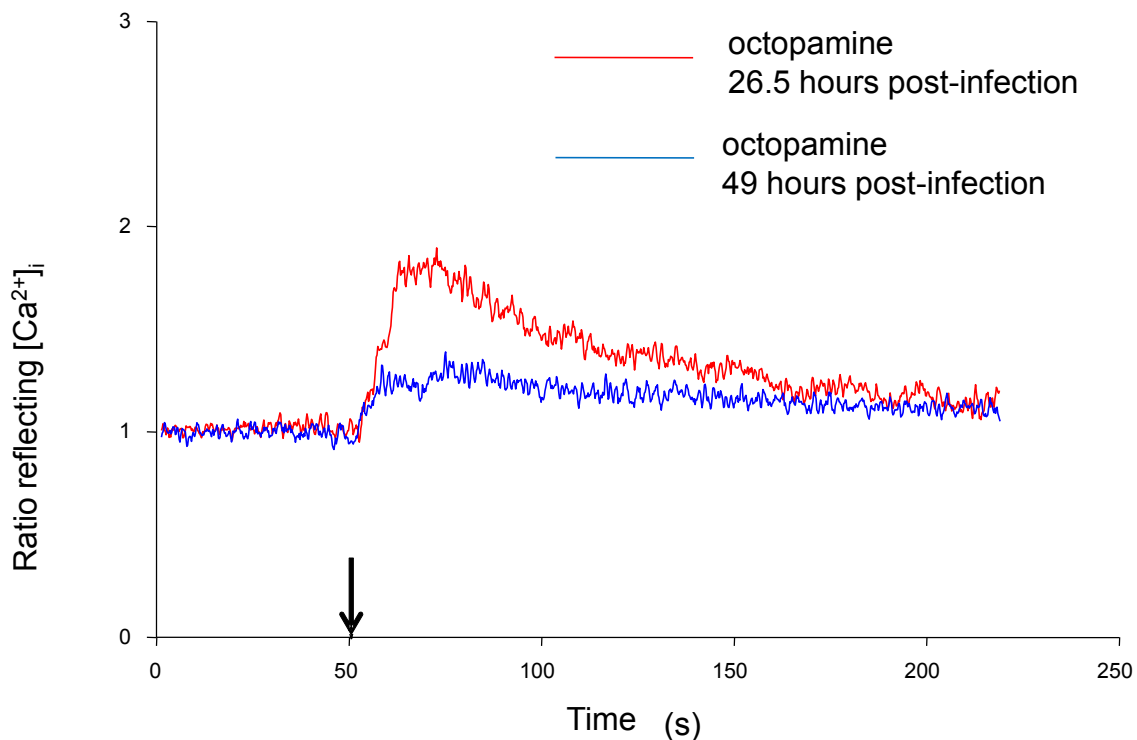


**Figure 10: Effect of infection time on intracellular  $\text{Ca}^{2+}$  concentration change in response to octopamine in baculovirus-Sf9 cells.** The experiment was conducted in the presence of extracellular  $\text{Ca}^{2+}$ . Each trace represents the response of a single Sf9 cell to the addition of 100  $\mu\text{M}$  octopamine at  $t=50$  seconds. Red trace: calcium transient in cell 26.5 hours post infection. Blue trace: calcium transient in cell 49 hours post infection. Data shown is representative of three identical experiments.

The Sf9-baculovirus system was shown to express significant levels of exogenous viral proteins as early as 22 hours following infection [60] and could be detected as far as 60 hours

post-infection (*data not shown*) . Experiments were performed between 25 and 48 hours post infection to ensure the cells were functional.

Control experiments were performed with the various agonists, inhibitors and modulators used throughout the course of this study on  $\text{Ca}^{2+}$  signalling in rPAR1-expressing Sf9 cells. Table 1 summarizes the qualitative changes observed when the various agents were added to wild-type Sf9 cells. The results obtained suggest that these compounds had no effect on wild-type Sf9 cells.

Agonist/inhibitor/modulator/vehicle	Qualitative change vs baseline in ratio representing $[\text{Ca}^{2+}]_i$	
	$\text{Ca}^{2+}$ -rich medium	$\text{Ca}^{2+}$ -free medium
octopamine (insect neurohormone agonist)	+++ (biphasic)	+++ (peak)
thrombin (PAR1 agonist)	n.e.	n.e.
PAR1-AP (PAR1 agonist)	n.e.	n.e.
$\text{La}^{3+}$ ( $\text{Ca}^{2+}$ channel & pump inhibitor)	n.e.	n.e.
nifedipine (L-type $\text{Ca}^{2+}$ channel inhibitor)	n.e.	n.e.
D-600 (voltage dependent $\text{Ca}^{2+}$ -inhibitor)	n.e.	n.e.
thapsigargin ( $\text{Ca}^{2+}$ -ATPase inhibitor)	+	+
TMB-8 ( $\text{IP}_3\text{R}$ - $\text{Ca}^{2+}$ channel inhibitor)	n.e.	n.e.
D-609 (PLC $\beta$ modulator)	n.e.	n.e.
bisindolylmaleimide (PKC modulator)	n.e.	n.e.
PDBu (PKC modulator)	n.e.	n.e.
H-89 (PKA modulator)	n.e.	n.e.
vehicles	n.e.	n.e.

**Table 1: Summary of qualitative changes in Fura-2 fluorescence ratio reflecting  $[\text{Ca}^{2+}]_i$  in control experiments.** Agonists, inhibitors, solvents or modulators were diluted in vehicle and added to wild-type Sf9 cells (n=3) in  $\text{Ca}^{2+}$ -rich or  $\text{Ca}^{2+}$ -free medium. Large biphasic responses in ratio reflecting calcium are indicated (+++). Slight increase (+) in  $[\text{Ca}^{2+}]_i$  is indicated. Slight increase with thapsigargin may due to a slight increase in cytosolic  $[\text{Ca}^{2+}]$  when the  $\text{Ca}^{2+}$ -ATPase is inhibited. Other agents, modulators and vehicles had no effect (n.e.) on the  $[\text{Ca}^{2+}]_i$  of cells.

### **3.3 Functional coupling of rPAR1 in Sf9 cells**

Once it was established that rPAR1 could be successfully expressed in Sf9 cells, the next step was to investigate whether this receptor could couple functionally to the Sf9 cell's signalling apparatus and, if so, to characterize the response to its agonist.

#### **3.3.1 Effect of thrombin**

In order to determine whether the rPAR-Sf9 possessed an exodomain highly similar to mammalian cells, that will bind and be activated by thrombin's serine protease activity, thrombin was used to stimulate the rPAR1-Sf9. Typical rPAR1-Sf9 responses are shown in Figure 11, which demonstrates functional coupling of the rPAR1 to  $\text{Ca}^{2+}$  signalling in the Sf9 cell, in the presence or absence of extracellular  $\text{Ca}^{2+}$ . The arrow indicates the time of addition of 10 U/ml of thrombin to a final volume of 1ml in the experimental chamber.

In the presence of extracellular  $\text{Ca}^{2+}$  (2.8GSM), thrombin produced a biphasic increase in intracellular calcium concentration, consisting of an initial surge followed by a slow return to baseline in a plateau-like fashion. In calcium-free medium (0GSM), only the first phase of the response was observed, consisting of the initial surge followed by a rapid return to baseline. The amplitude differences noted in the ratio is due to variability in individual single cell responses.

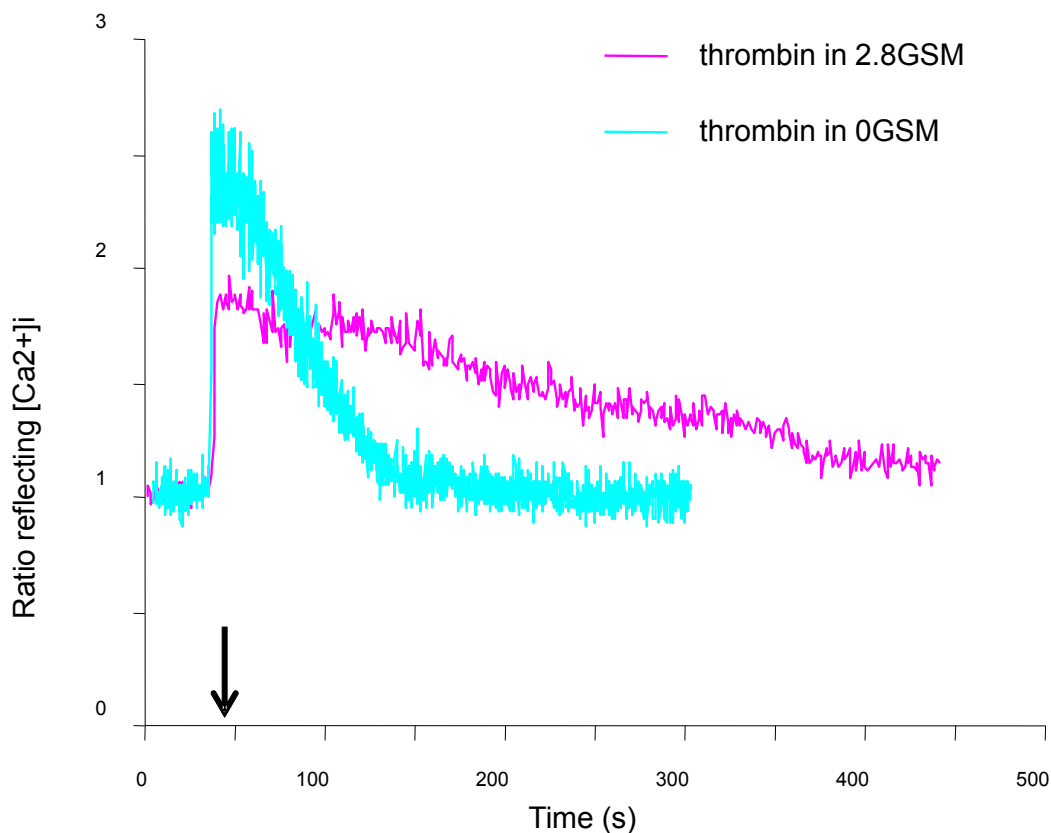


**Figure 11: Effect of thrombin on  $[Ca^{2+}]_i$  in Sf9 insect cells expressing rPAR1.** The functional coupling of rPAR1 to the  $Ca^{2+}$  signalling apparatus of the Sf9 cell system is apparent by the calcium surge which follows the addition of 10U/ml of thrombin (arrow) to the Sf9-rPAR1 cell. The initial surge in  $[Ca^{2+}]_i$  is comparable in both calcium-free (turquoise trace) and calcium-containing (pink trace) media, but when  $Ca^{2+}$  is present in the extracellular space, a plateau follows the initial phase.

### 3.3.2 Effect of PAR1-AP

In mammalian cells, PAR1-AP, a small, 5 amino acid peptide (Ser-Phe-Leu-Leu-Arg), identical to the minimal region of the truncated N-terminus of the thrombin-cleaved PAR1, acts as an agonist to the receptor [20]. The activity of PAR1-AP was tested on PAR1 Sf9 cells to confirm whether the ligand binding sites present on the receptor exodomain were held in a conformation consistent with that in mammalian cells. Figure 12 shows that the PAR1-AP triggered responses which were similar to those obtained with thrombin: an initial  $[Ca^{2+}]_i$

surge was followed by a plateau phase in 2.8GSM, whereas the response to PAR1-AP comprised only the initial  $[Ca^{2+}]_i$  surge in 0GSM.

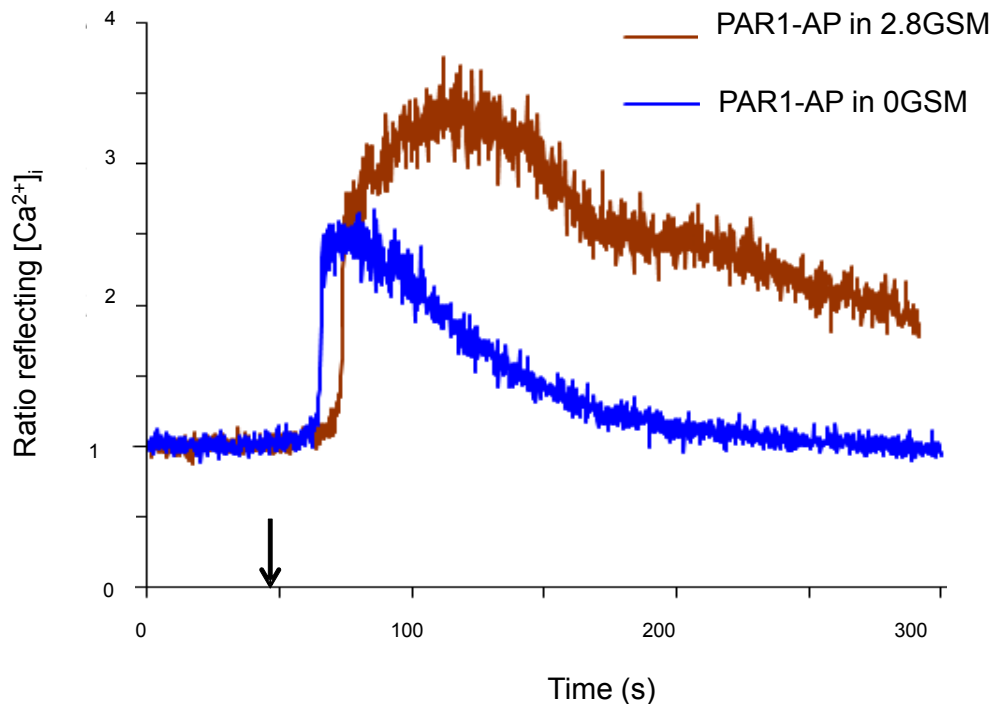


**Figure 12: Effect of synthetic peptide PAR1-AP on  $[Ca^{2+}]_i$  in rPAR1-Sf9 cells.** The addition of 50  $\mu$ M PAR1-AP (arrow) yielded a response which was qualitatively similar to those produced by the addition of thrombin. The maroon trace demonstrates the typical biphasic response obtained in calcium containing medium, whereas the blue line demonstrates the response obtained in a calcium-free medium.

Overall, the intracellular  $Ca^{2+}$  concentration changes produced following either thrombin or PAR1-AP addition were comparable in their kinetics. In 2.8GSM, the agonists produced an initial large peak in the intracellular  $Ca^{2+}$  level, within 10 seconds of the addition of agonist. The intracellular  $Ca^{2+}$  signal then decreased somewhat, but remained sustained in a plateau phase and remained high for up to 6 minutes. In the presence of external  $Ca^{2+}$  the surge was generally greater. In the absence of extracellular  $Ca^{2+}$  (0GSM), the plateau phase

was not observed and instead, intracellular calcium concentration levels returned rapidly to the initial level.

### **3.4 Modulation of the rPAR1-Sf9 cell signal**

The experiments described above demonstrated that the rPAR1-Sf9 expression system yielded a receptor protein functionally similar to that found in mammalian cells, in terms of responsiveness to thrombin and PAR1-AP. Therefore, the receptor could be studied, isolated from other mammalian receptors, using the Sf9-baculovirus expression system.

While PAR1-AP has been shown to activate PAR1 at concentrations of 0.5-6  $\mu\text{M}$  [4], dose-response curves were not attempted, instead, to achieve full activation of the  $\text{Ca}^{2+}$  signalling process in rPAR1-Sf9 cells, supra-maximal doses of PAR1-AP, i.e. 50-100 $\mu\text{M}$ , were used in all experiments described in the following sections.

#### **3.4.1 Effect of calcium-channel inhibitors**

By examining the results we obtained by rPAR1 stimulation by thrombin or PAR1-AP in calcium-deficient and calcium-rich conditions, we believed that the  $\text{Ca}^{2+}$  response was a biphasic process characterized by a release of  $\text{Ca}^{2+}$  from internal stores coupled to an influx dependent on the presence of  $\text{Ca}^{2+}$  outside the cells.

In order to study the mechanisms involved in  $\text{Ca}^{2+}$  influx into the cells, various plasma membrane calcium inhibitors were used, either before or after the stimulation of the cells by PAR1-AP in the presence of extracellular  $\text{Ca}^{2+}$ . The effects of  $\text{La}^{3+}$  ions, nifedipine and D-600 are described in the following sections.



### 3.4.1.1 Effect of lanthanum

$\text{La}^{3+}$  is a widely used inorganic calcium influx inhibitor. Results shown in Figure 13 show that pre-incubation of rPAR1-Sf9 cells with 5mM  $\text{La}^{3+}$  caused a rapid return to the baseline  $[\text{Ca}^{2+}]_i$  when PAR1-AP was added. This pre-incubation with 5mM  $\text{La}^{3+}$  yielded a PAR1-AP response similar to what was obtained in a calcium-free solution.

When rPAR1-Sf9 cells were stimulated with PAR1-AP,  $\text{La}^{3+}$  could be added within seconds (Figure 15), and will also truncate the second phase of the response and cause a more rapid return to baseline.

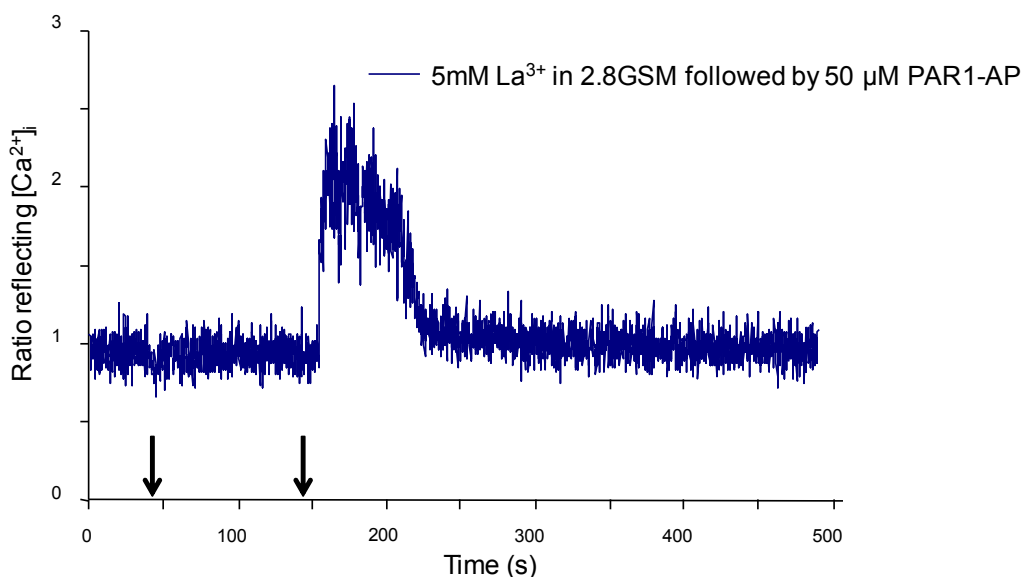


**Figure 13: Effect of  $\text{La}^{3+}$  pre-incubation on the  $[\text{Ca}^{2+}]_i$  response to PAR1-AP.**

The figure demonstrates the effect of the addition of 5mM  $\text{La}^{3+}$  at 45 seconds (first arrow) followed by 50  $\mu\text{M}$  PAR1-AP at 145 seconds. Addition of 50 $\mu\text{M}$  PAR1-AP is indicated by the second arrow.  $\text{La}^{3+}$  in a  $\text{Ca}^{2+}$ -rich medium prevents the entry of  $\text{Ca}^{2+}$  from the extracellular space and yields a response that is similar to what is typically seen in the absence of extracellular  $\text{Ca}^{2+}$ .

While  $\text{La}^{3+}$  is widely used as a general, or non-specific,  $\text{Ca}^{2+}$  channel and influx inhibitor, Sf9 cells are known to specifically possess voltage-dependent and L-type  $\text{Ca}^{2+}$  channels [40].

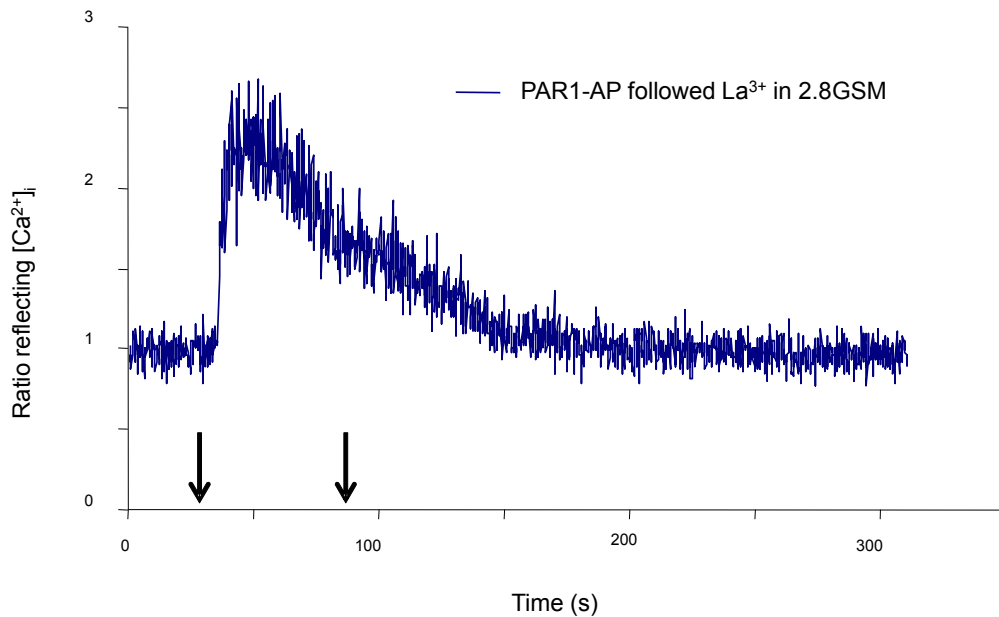


**Figure 14: Effect of  $\text{La}^{3+}$  applied during the  $[\text{Ca}^{2+}]_i$  surge triggered by PAR-AP.** Addition of  $100\mu\text{M}$  PAR1-AP (first arrow) followed by  $5\text{mM}$   $\text{La}^{3+}$  (second arrow). The inhibition of  $\text{Ca}^{2+}$  channels truncated the typical response to PAR1-AP.

The role of these  $\text{Ca}^{2+}$  channels in the  $\text{Ca}^{2+}$  response following heterologous receptor expression has not been definitively demonstrated [70]. The possible involvement of these channels in the plateau phase was therefore further assessed using nifedipine and D-600.

#### 3.4.1.2 Effect of nifedipine

Nifedipine is a dihydropyridine known to specifically inhibit L-type calcium channels [71]. Figure 15 demonstrates that nifedipine interfered with the second phase of the  $\text{Ca}^{2+}$  response demonstrating a the contribution of  $\text{Ca}^{2+}$  channels to this component of the response.

Addition of PAR1-AP followed closely by nifedipine yielded a PAR1-AP response similar to what was seen in calcium free experiments (Figure 15), suggesting that the second phase of the response was mediated by the activation of L-type calcium channels.

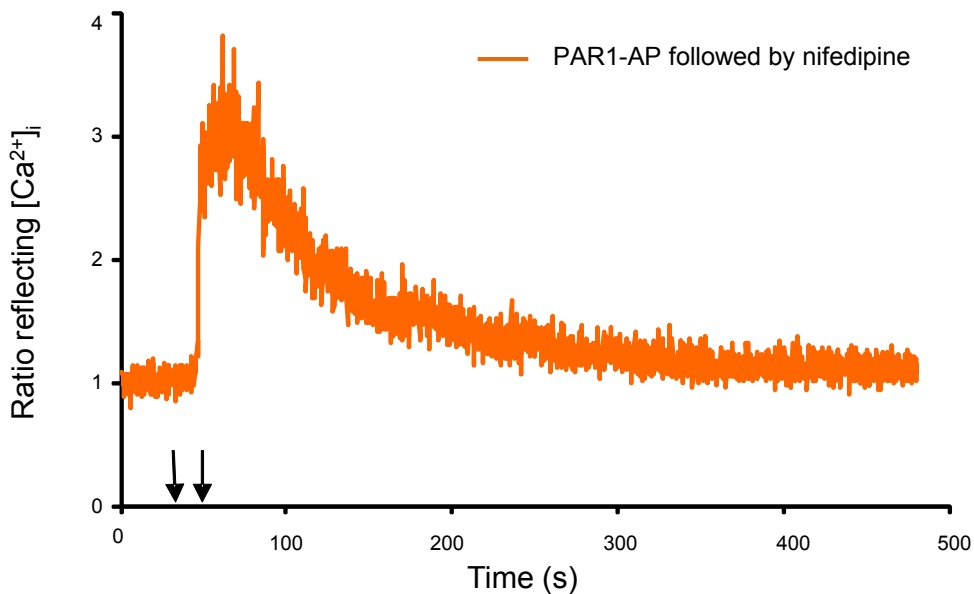


**Figure 15: Effect of nifedipine on the  $\text{Ca}^{2+}$  flux produced by PAR1-AP activation in rPAR1-Sf9 cells.** Orange trace represents  $100\mu\text{M}$  PAR1-AP at 50 seconds followed by  $10\mu\text{M}$  nifedipine at 75 seconds in the presence of extracellular  $\text{Ca}^{2+}$ .

Addition of PAR1-AP followed closely by nifedipine yielded a PAR1-AP response similar to what was seen in calcium free experiments (Figure 15). This result suggests that the second phase of the  $\text{Ca}^{2+}$  response was mediated by the activation of L-type calcium channels. This is, however, no effect of nifedipine on the action of  $\text{IP}_3\text{R}$   $\text{Ca}^{2+}$  channels as its action is restricted to the  $\text{Ca}^{2+}$  channels present in the plasma membrane.

### 3.4.1.3 Effect of D-600

D-600 is a lipophilic, organic voltage-dependent calcium-channel blocker. This agent can exercise its action intracellularly as well as extracellularly [71]. Use of D-600 after cell stimulation by PAR1-AP induced oscillations during the plateau phase of the  $[\text{Ca}^{2+}]_i$  response (Figure 16, green trace). On the other hand, pre-incubation with D-600 caused a full inhibition of the PAR1-AP response (Figure 16, blue trace).

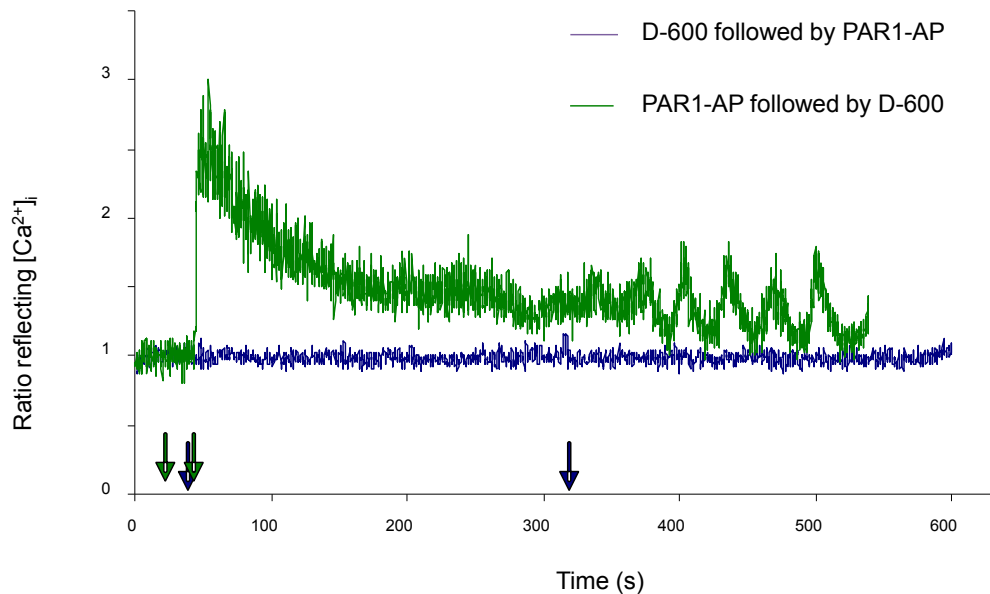


**Figure 16: Effect of D-600 on the  $[Ca^{2+}]_i$  response to PAR1-AP .** Attenuation of the PAR1-AP response occurs following incubation of cells with  $100\mu M$  D-600 (blue trace), the first arrow indicates addition of D-600 while the second arrow indicates of the addition of PAR1-AP. The green trace shows the addition of  $100\mu M$  PAR1-AP (first green arrow) quickly followed with D-600 (second green arrow) in a  $Ca^{2+}$  containing environment.

The results obtained (Figure 16) suggest that in rPAR1-Sf9, incubation of cells with D-600 allows it to act as an intracellular  $Ca^{2+}$  channel blocker similar to TMB-8. Oscillations caused by the addition of D-600 immediately following PAR1-AP suggests that D-600 interferes with the return to baseline  $[Ca^{2+}]_i$ .

### 3.4.2 Effect of other calcium transport modulators

Once it was established that the second phase of the intracellular  $Ca^{2+}$  surge observed in response to thrombin and PAR1-AP stimulation was likely due to the influx of extracellular  $Ca^{2+}$  through L-type  $Ca^{2+}$ -channels of the plasma membrane of the cells, experiments were conducted to determine what was responsible for the initial phase of the surge observed in calcium-free solution or in the presence of calcium transport blockers.

### 3.4.2.1 Effect of thapsigargin

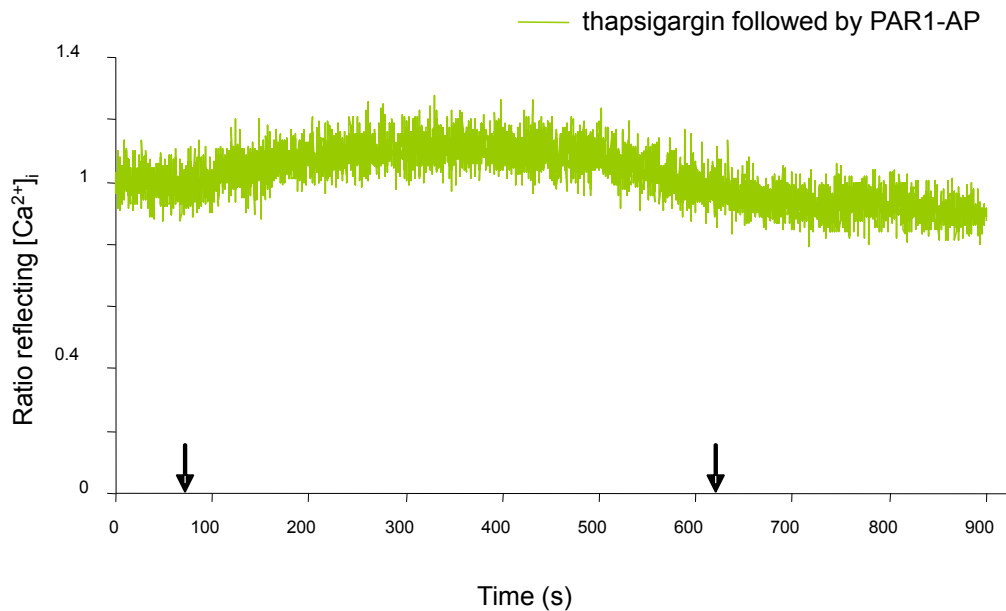


**Figure 17: Effect of thapsigargin on the [Ca<sup>2+</sup>]<sub>i</sub> response to PAR1-AP activation in rPAR1-Sf9 cells.** Addition of 100nM thapsigargin (first arrow) is followed by a slow increase in [Ca<sup>2+</sup>]<sub>i</sub> as Ca<sup>2+</sup> passively exits the ER, travelling down the concentration gradient. The addition of 100μM PAR1-AP (second arrow) does not produce any increase in [Ca<sup>2+</sup>]<sub>i</sub>.

Thapsigargin is a calcium-ATPase inhibitor which inhibits calcium resequestration in intracellular Ca<sup>2+</sup> storage sites. Thapsigargin is also known to cause an influx of Ca<sup>2+</sup> from extracellular space in the absence of any phosphoinositide hydrolysis, a phenomenon prevented here by the use of calcium-free medium. As shown in Figure 17, the 5-minute incubation of rPAR1-Sf9 cells with 100nM thapsigargin in calcium-free medium caused a slight surge in [Ca<sup>2+</sup>]<sub>i</sub> immediately following the addition of thapsigargin to the experimental chamber, as has been reported previously [72]. Pre-treatment with thapsigargin completely abolished the [Ca<sup>2+</sup>]<sub>i</sub> surge normally induced by the PAR1-AP peptide, as described above.

### 3.4.2.2 Effect of TMB-8

TMB-8 is an IP<sub>3</sub>R-Ca<sup>2+</sup> channel antagonist which prevents the release of Ca<sup>2+</sup> from internal stores, the ER in particular. Pretreatment with 100 μM TMB-8 inhibited the PAR1-AP effect in 50% of the rPAR1 expressing cells tested in 2.8GSM (Figure 18 and Figure 19).

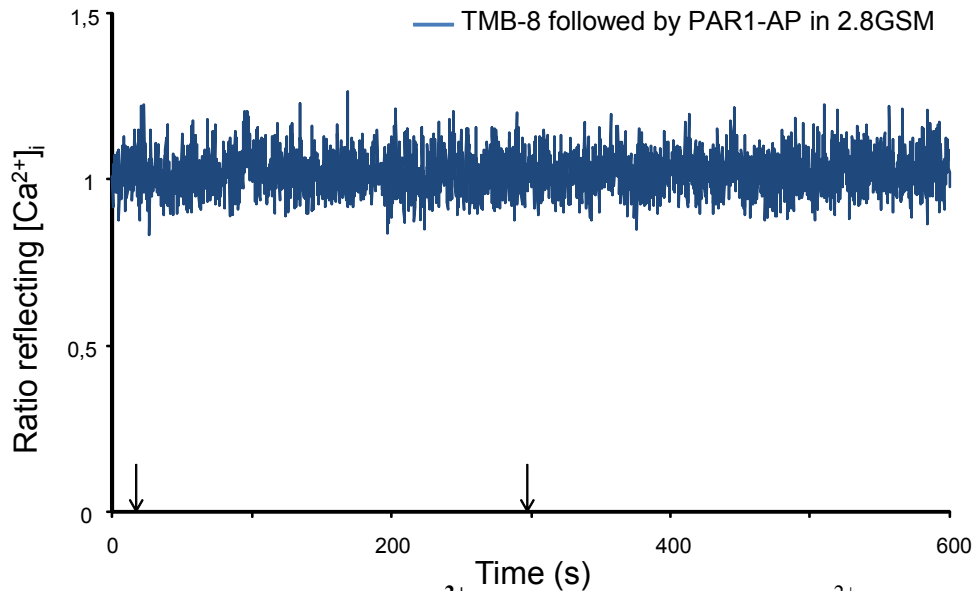


**Figure 18: TMB-8 inhibition of Ca<sup>2+</sup> release from the ER.** In Ca<sup>2+</sup>-rich media, 100μM TMB-8 inhibited the Ca<sup>2+</sup> transient normally produced by 50 μM PAR1-AP. No change in ratio reflecting Ca<sup>2+</sup> was anticipated, but was only seen in 50% of the cells tested.

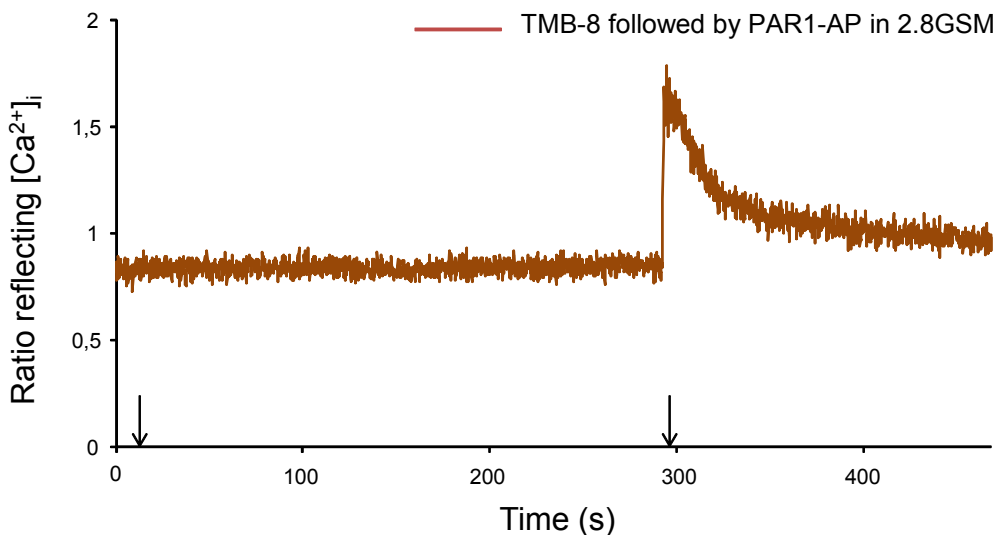


**Figure 19. Ineffective inhibition by TMB-8.** 100μM TMB-8 did not consistently inhibit the Ca<sup>2+</sup> transient produced by 50μM PAR1-AP in Ca<sup>2+</sup>-containing media.

It was noted that in experiments in which the PAR1-AP response was abolished in 2.8GSM, a minimum 5-minute pre-incubation period with TMB-8 was required to inhibit the  $\text{Ca}^{2+}$  transient entirely.

In the absence of extracellular  $\text{Ca}^{2+}$ , 100% of the cells tested showed total suppression of the calcium transient produced by PAR1-AP, therefore, similar to Figure 18A, no change to the ratio reflecting  $[\text{Ca}^{2+}]_i$ , even when incubated with TMB-8 for short periods of time (between 250 and 300 seconds). The results suggest that the  $\text{Ca}^{2+}$  surge was indeed made of  $\text{Ca}^{2+}$  release from internal stores, particularly the ER.

It is difficult, however, to conclude whether TMB-8 is an effective signal modulator in Sf9 cells as responses lacked consistency but previous studies have successfully used TMB-8 as a  $\text{IP}_3\text{R-Ca}^{2+}$  channel inhibitor.

### **3.4.3 Signal cascade modulation**

The results described in the preceding sections demonstrated that the  $\text{Ca}^{2+}$  surge triggered by PAR1 activation was made of two components: the influx of extracellular  $\text{Ca}^{2+}$  and the release of  $\text{Ca}^{2+}$  from internal stores. The following sections are devoted to further studies aimed at exploring the components of the signalling cascade involved in the PAR1-AP induced response.

#### **3.4.3.1 Effect of D-609**

D-609 is a  $\text{PLC}\beta$  inhibitor [73]. In order to determine the role of  $\text{PLC}\beta$  in the  $[\text{Ca}^{2+}]_i$  surge in response to PAR1-AP stimulation, D-609 was used. Figure 20 shows that regardless of the presence or absence of extracellular calcium, the response elicited by PAR1-AP was not affected by the addition of  $100\mu\text{M}$  D-609 five minutes prior to the addition of  $50\mu\text{M}$  PAR1-

AP, suggesting that PLC $\beta$  does not appear to be involved in the pathway linking PAR1 to the release of Ca<sup>2+</sup> from intracellular stores.

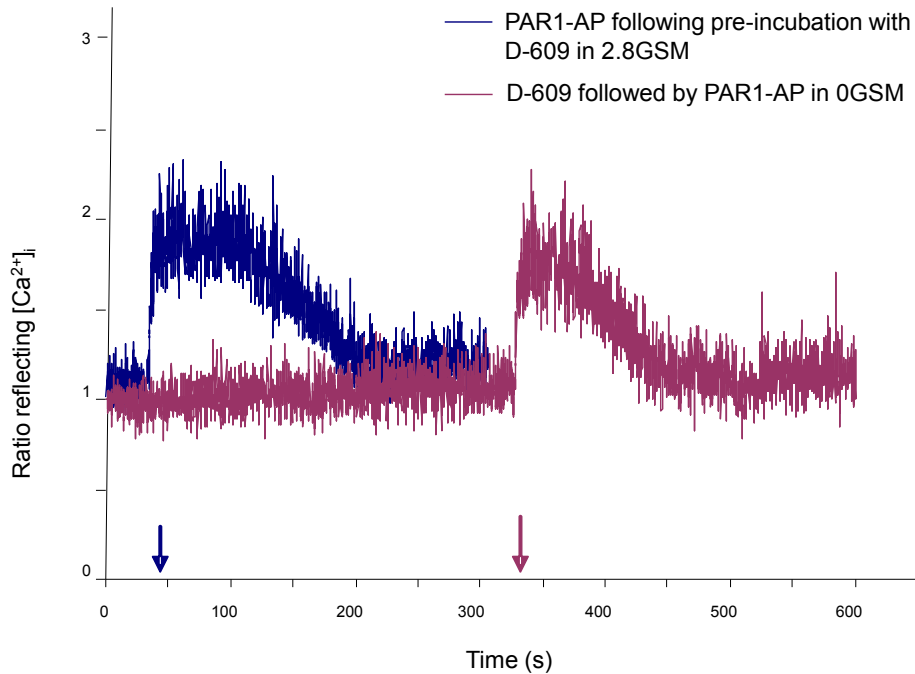


**Figure 20: Effect of D-609 on the [Ca<sup>2+</sup>]<sub>i</sub> response to PAR1-AP.** In Ca<sup>2+</sup>-free medium (purple trace), rPAR1-Sf9 cells were incubated with 100  $\mu$ M D-609 for 5 minutes followed by the addition of 50  $\mu$ M PAR1-AP (purple arrow). In a Ca<sup>2+</sup>-rich environment (blue trace) shows a cell previously incubated for 5 minutes and the addition of 50  $\mu$ M PAR1-AP (blue arrow).

### 3.4.3.2 Effect of protein kinase modulators

#### 3.4.3.2a Effect of bisindolylmaleimide

As mentioned in section 1.3, PAR1 coupling to G $\alpha_q$  activates PLC $\beta$  with the subsequent formation of IP<sub>3</sub> and DAG. The DAG pathway will lead to downstream activation of PKC which ultimately replenishes the G $\alpha_q$  substrate pool. Bisindolylmaleimide has been shown to interfere in this signalling cascade through the inhibition of PKC [43]. This inhibition depletes the PLC $\beta$ 's substrate pool.



The effect of bisindolylmaleimide on the  $[Ca^{2+}]_i$  signal varied with the experimental conditions. As shown in Figure 21, in a  $Ca^{2+}$ -free medium, addition of 200nM of the inhibitor prior to that of PAR1-AP significantly blunted the  $Ca^{2+}_i$  signal. On the other hand, this compound used in the presence of extracellular  $Ca^{2+}$  did not affect the magnitude of the response to PAR1-AP, but it induced oscillations following the initial surge.

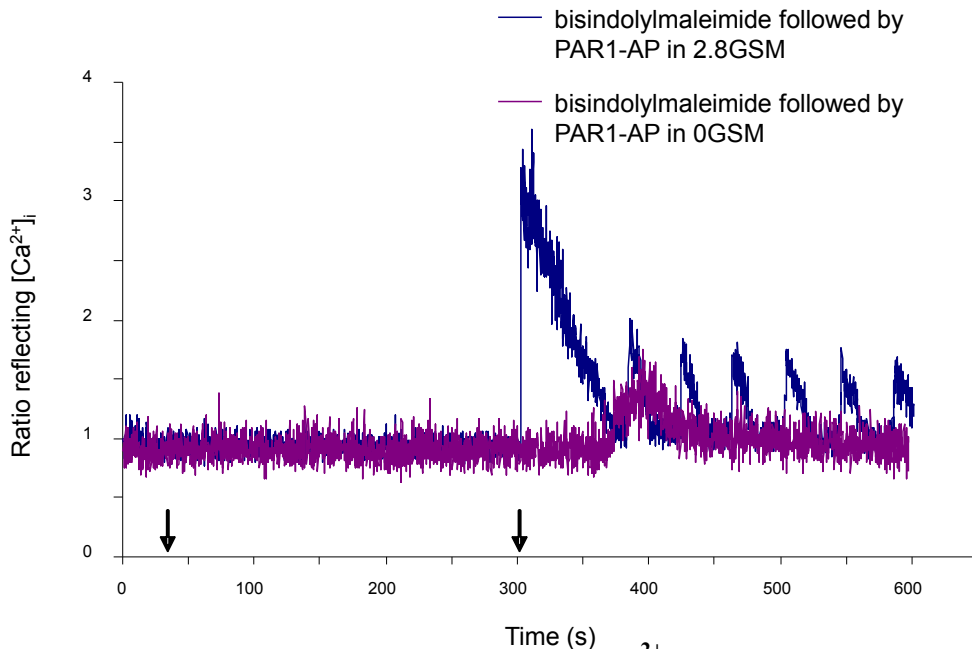


**Figure 21: Effect of bisindolylmaleimide on the  $[Ca^{2+}]_i$  response induced by PAR1-AP.** Incubation of rPAR1-Sf9 cells with 200nM bisindolylmaleimide followed by 100 $\mu$ M PAR1-AP in  $Ca^{2+}$ -free environment (purple trace). In a  $Ca^{2+}$ -rich medium, 200nM bisindolylmaleimide followed by 100 $\mu$ M PAR1-AP shows a large  $Ca^{2+}$  flux followed by rapid decrease in intracellular  $Ca^{2+}$  and  $[Ca^{2+}]_i$  oscillations (blue trace).

### 3.4.3.2b Effect of PDBu

PDBu is a protein kinase C activator [44]. Figure 22 (blue trace) shows that the second phase of the PAR1-AP-induced  $Ca^{2+}$  response in 2.8GSM was significantly reduced in the presence of PDBu. However, in the absence of extracellular  $Ca^{2+}$ , rPAR1-Sf9 cells incubated in PDBu did not respond to PAR1-AP stimulation (Figure 22, brown trace).

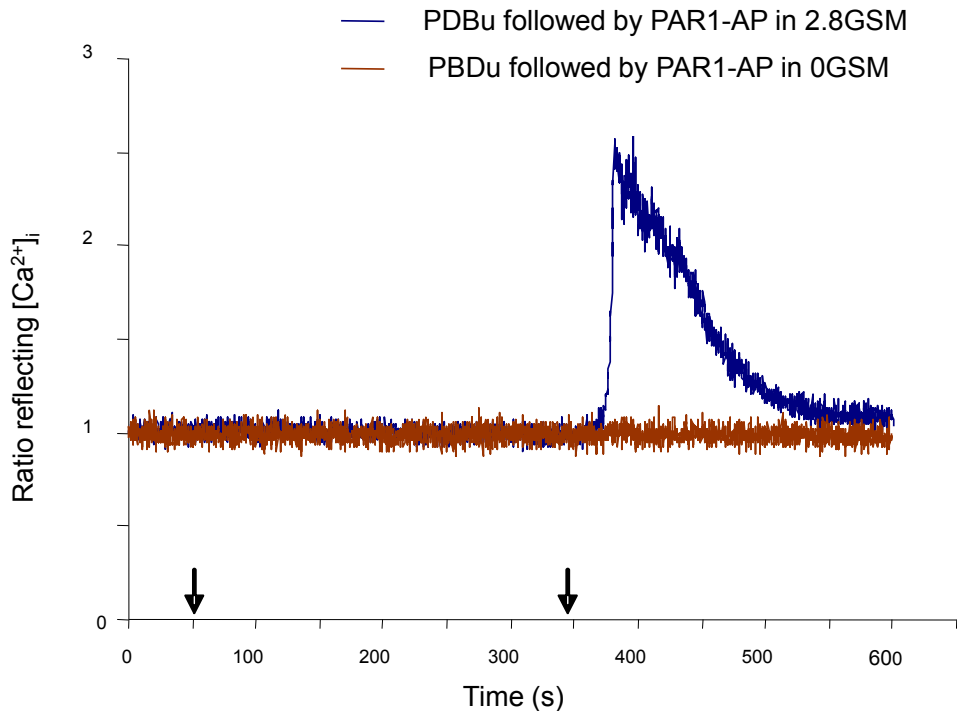


**Figure 22: Effect of PDBu on the Ca<sup>2+</sup> surge produced by PAR1-AP.** Incubation with 200nM PDBu for 5 minutes (at 50 seconds, first arrow) followed by the addition of 50 $\mu$ M PAR1-AP (at 350 seconds, second arrow). The blue trace shows an attenuated response to PAR1-AP with virtually no second or plateau phase in calcium-rich medium. The brown trace shows that incubation with PDBu suppressed the Ca<sup>2+</sup> surge in Ca<sup>2+</sup>-free environment.

Altogether, the results from the experiments conducted with PKC modulators demonstrate that this kinase plays an active role in the Ca<sup>2+</sup> signalling pathway activated by rPAR1.

### 3.4.3.2c Effect of H-89

H-89 is a PKA inhibitor that is believed to competitively bind to the ATP binding site on the catalytic subunit of PKA, thereby interfering with the G<sub>i</sub>/G<sub>s</sub>-AC pathway, by blocking the phosphorylation of PKA [74]. Figure 23 shows that in cells pre-incubated with H-89, an increase in plateau duration was observed in response to PAR1-AP in a Ca<sup>2+</sup>-rich environment. On the other hand, incubation of the cells with this compound resulted in

the complete inhibition of the PAR1-AP response in  $\text{Ca}^{2+}$ -free environment. This data clearly demonstrates the involvement of PKA in the  $[\text{Ca}^{2+}]_i$  signalling cascade. Whereas H-89 had a substantial effect on the  $\text{Ca}^{2+}$  signal induced by PAR1-AP, recent uncertainty about the activity of H-89 [37] makes it impossible to decipher what mechanism is affected by this agent.

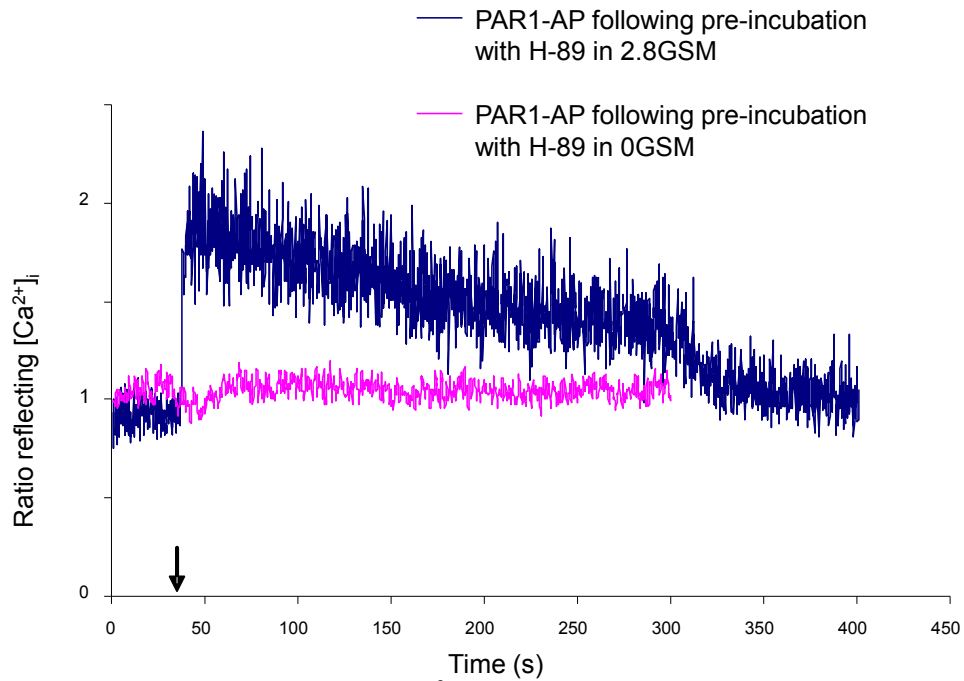


**Figure 23: Effect of H-89 on the  $[\text{Ca}^{2+}]_i$  response to PAR1-AP.** Addition of 100 $\mu\text{M}$  PAR1-AP in rPAR1-Sf9 cells preincubated with 500nM H-89 in a  $\text{Ca}^{2+}$ -rich medium (blue trace) and  $\text{Ca}^{2+}$ -free medium (pink trace). Arrow indicates the addition of 100  $\mu\text{M}$  PAR1-AP in both cases.

## **DISCUSSION**

Thrombin's proteolytic action is a critical step in the coagulation cascade. Whereas historically, thrombin's role in cleaving fibrinogen was considered its exclusive action, the receptor-mediated activity of thrombin allows it to act on a variety of cellular targets. A number of thrombin receptors have been identified, including PAR1 [4].

On the other hand, Sf9 cells have become one of the most used cell lines for recombinant protein expression due to their versatility and the high expression levels that can be achieved.

For this work, the Sf9 recombinant baculovirus expression system was successfully used to induce the virus-mediated delivery of foreign proteins into Sf9 cells in an efficient and relatively simple expression system. Effective functional coupling of the PAR1 to Sf9 signalling apparatus was demonstrated through  $\text{Ca}^{2+}$  assaying, and modulation of various signalling components provided insight into the downstream mediators of the  $\text{Ca}^{2+}$  mobilization following stimulation with PAR1-AP in the rPAR1-Sf9 cells.

#### **4.1 Sf9-Baculovirus expression system**

The findings of this study confirm the successful expression of PAR1 in Sf9 cells using the baculovirus expression system.

Sf9 cells have been extensively used for exogenous protein expression and have been studied for this purpose. Exogenous receptors expressed using this cell system yield GPCRs with similar post-translational modifications and comparable pharmacology to native mammalian proteins, with differences mainly noted in N-glycosylation [75].

Sf9 cells possess one G-protein form of  $G\alpha_i$ , and both  $G\alpha_q$  and  $G\alpha_s$ -like proteins, as well as PLC and AC [40]. Only Sf9  $G\alpha_q$ , and  $G\alpha_s$  have been shown to be activated by

exogenous receptors expressed using the Sf9-recombinant baculovirus system,  $G\alpha_i$  does not typically couple with most mammalian receptors [76].

There are some limitations to this expression system. Sf9 cells lack the ability to fully glycosylate proteins. Indeed, rPAR1 expressed in this cell system yielded a receptor with slightly lower molecular mass than that seen in mammalian cells [75].

While endogenous receptors of Sf9 do not interfere with exogenous mammalian receptors, receptor densities, relatively limited availability due to low levels of endogenous G-protein and receptor/G-protein stoichiometry may influence functional coupling [70].

The baculovirus expression system uses a genetically modified baculovirus whereby the exogenous protein gene is inserted distal to the polyhedrin promoter. The pathological processes inherent to the use of recombinant baculovirus can be limitations to the use of this system. For instance, one disadvantage of polyhedrin promoter mediated recombinant baculovirus use is that the polyhedrin promoter is expressed late in the infection cycle, when cells start to lyse [75].

While reduced viability could be expected as a consequence of baculovirus infection, assays which were conducted with recombinant-PAR1 and wild-type baculovirus demonstrated that only recombinant baculovirus infected Sf9 cells tended to respond poorly to octopamine as infection progressed. The results obtained suggest that the pathological state does not contribute to the attenuation of the  $Ca^{2+}$  response in infected Sf9 cells as was previously suggested [75], but that either the expression of exogenous receptor, competitive coupling of exogenous G-protein coupled rPAR1 and endogenous octopamine receptor, or the localization of rPAR1 on the cell membrane interfere with the octopamine receptor activation of a  $Ca^{2+}$  response.

Altogether it was established that although the octopamine response in Sf9 cells was a reliable viability test using microspectrofluorescence, qualitative, as opposed to quantitative differences in the  $\text{Ca}^{2+}$  fluxes should be noted. Optimal Sf9 cell functionality was determined to be between 25 and 48 hours following infection with recombinant baculovirus.

The rPAR1-Sf9 system presented several challenges throughout this study. In addition to those discussed above, the baculovirus-Sf9 cell system proved to have several other limitations. For instance, the system was non-functional during summer months (June, July and August) for unknown reasons. While cell cultures and infection with recombinant baculovirus were performed in a controlled environment throughout the year, it was difficult to consistently prove the viability of cells during summer months. This system was very sensitive to minor fluctuations in seasonal changes, humidity, fungus and bacterial contamination, a finding supported by other groups [40].

Recent recommendations include the use of single-use polycarbonate Erlenmeyer bottles for cell propagation [75], however such a recommendation is relatively new. Experts within the Biotechnology Research Institute were consulted and staff was instructed to re-initiate cell cultures periodically, and maintain them between 6 and 65 passages. This proved to be an additional source of delay in the study.

A possibility for future study would be to elaborate a stably transformed cell line where no pathological process and no cell lysis would occur [77].

#### **4.2 Effective coupling of rPAR1 and modulation of response in Sf9 cells**

The basis of PAR1 activation by thrombin through the generation of a tethered ligand has implications with regard to the kinetics and magnitude of cellular response. Dose-dependent responses to thrombin have been demonstrated [78], but given that a single

thrombin molecule can cleave and activate numerous receptors, it may be possible that given enough time, one single molecule could cleave enough receptors to induce a response of greater magnitude.

Once cleaved and activated by thrombin, PAR1 undergoes PKC-dependent [45, 79, 80] and PKC-independent, G-protein receptor kinase-dependent phosphorylation at its C-terminal Ser and Thr residues in order to inactivate the receptor [4]. Synthetic peptides corresponding to a five amino acid peptide sequence capable of activating the receptor and its downstream signalling cascades have been shown to prolong the activity of PAR1 [81]. The shortest peptide sequence shown to activate PAR1 corresponds to Ser-Phe-Leu-Leu-Arg and is known as PAR1-AP. Receptor activation is quickly followed by its phosphorylation and lysosomal sequestration. Lysosomal degradation is reserved to a portion of activated PAR1 while some receptors return to the cell surface [79] where they remain inactive.

Resensitization to thrombin depends on a pool of naive receptors located intracellularly which have been defined in a number of cell types [4, 9]. Due to the irreversible nature of thrombin activation of the receptor, PAR1-AP was selected as the preferred agonist. This peptide sequence binds reversibly to the receptor's active site and dissociation allows PAR1 to remain functional [19].

For the current work, the use of microspectrofluorescence allowed for the study of the  $\text{Ca}^{2+}$  signalling pathway activated through exogenous receptor expression in Sf9 cells. Figure 24 presents a schematic summary of the findings from our study of rPAR1 expressed using the Sf9-recombinant baculovirus system.



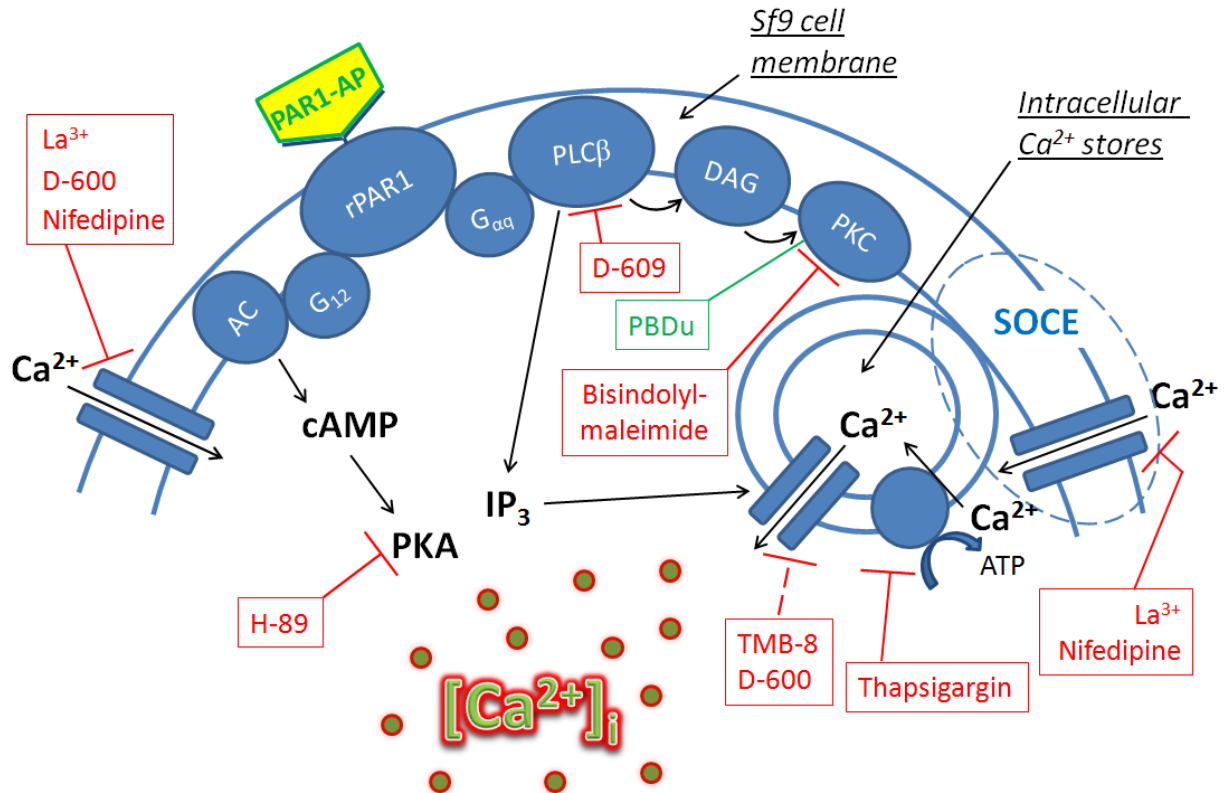


**Figure 24:  $\text{Ca}^{2+}$  signal modulation in rPAR1-Sf9.** Inhibitors and signal modulators used to determine the components which affect the  $[\text{Ca}^{2+}]_i$  signal in rPAR1 expressing Sf9 cells are schematically represented. Red text indicates an inhibitory function while green text is indicative of stimulatory function. SOCE represents the system of store-operated calcium entry including the translocation of STIM-1 to the puncta and activation of Orai-1 channels (as described in section 1.3.2 and discussed below).

While previous studies suggested the lack of a thrombin cleavage site in rPAR1-Sf9 [81], similar to work conducted by Chen & al [82], the current work demonstrated the successful expression of a functionally coupled rPAR1 which could be activated by both thrombin and PAR1-AP. Assays using confocal microscopy demonstrated that receptors were located mainly at the cell surface of PAR1-Sf9 cells.

Although Sf9 cells are known to possess a number of signal transduction components including  $G_{\alpha_{q,i,s,o}}$  as well as PLC and AC, the technique used in this study is limited to studying the impact of modulators exclusively on the mobilization of intracellular  $\text{Ca}^{2+}$ . Since

PAR1 has not been shown to couple to  $\alpha_o$  in mammalian cells [9], coupling to this G-protein was not explored as there would be limited clinical relevance .

In mammalian cells PAR1 couples to  $\alpha_{12/13}$  [9]. However that signal pathway is not known to have any effect on  $[Ca^{2+}]_i$ , so it was determined that the most likely G-protein subunits involved in generating a  $Ca^{2+}$  signal would be  $\alpha_q$  and  $\alpha_{i/z}$ .

rPAR1 coupling to  $G\alpha_q$  is the prerequisite for activation of the PLC $\beta$  (PLC $\beta$ ) signalling cascade and subsequent release of  $Ca^{2+}$  from intracellular pools [83], such as the ER. In this work, D-609 [73] was used to determine what role PLC $\beta$  played in the initial  $[Ca^{2+}]_i$  surge resulting from PAR1-AP addition. It was found that the inhibition of PLC $\beta$  by D-609 did not affect the rPAR1-Sf9 cell's release of  $Ca^{2+}$  from intracellular storage sites in response to PAR1-AP. These results could suggest that insect cell PLC $\beta$  is not sensitive to D-609.

Subsequent interference with downstream modulators was more revealing in that it could help determine whether modulation of the PLC signalling cascade further downstream could better define the role of this pathway.

It is known that activation of PLC $\beta$  leads to the hydrolysis of PIP $_2$  into IP $_3$  and DAG. DAG then leads to activation of PKC. Inhibition of PKC by bisindolylmaleimide [43] prevented the action of this effector mechanism, prolonging PAR1 receptor mediated activity [45]. Assays conducted as part of this work, in  $Ca^{2+}$  free medium, demonstrated that PAR1-AP could continue to induce the first phase of the  $Ca^{2+}$  response following incubation with bisindolylmaleimide. Furthermore, PAR1-AP addition to rPAR1-Sf9 cells treated with bisindolylmaleimide in the presence of extracellular calcium caused oscillations which may be indicative of continued receptor activation brought on by a lack of PKC which interferes with resequestration of  $Ca^{2+}$  in the intracellular stores.

Activation of PKC with PDBu [44, 45] enhances the phosphorylation of PAR1, thereby accelerating inactivation of the receptor and inhibiting the  $\text{Ca}^{2+}$  response.

Taken together, the findings from this work indicate a critical role for this DAG-PKC pathway in PAR1. Therefore, in rPAR1-Sf9, PKC activation seems to be an integral component of the plateau phase of the PAR1-AP  $\text{Ca}^{2+}$  response, as well as the resequestration of  $\text{Ca}^{2+}$ .

Since evidence indicates that Sf9 cells possess both  $\text{G}\alpha_q$  as well as  $\text{PLC}\beta$  [75], the fact that D-609 did not affect the rPAR1-Sf9's ability to activate a  $\text{Ca}^{2+}$  signal may point to limitations in this expression system. Previous studies have shown that PAR1 couples to endogenous  $\text{G}\alpha_q$  in Sf9 cells [26], but insect  $\text{G}\alpha_q$  is obviously not the physiological coupling partner of mammalian PAR1. Therefore, the impact of insect  $\text{G}\alpha_q$  on receptor pharmacology cannot be excluded. It is possible that the release of  $\text{Ca}^{2+}$  from the storage sites is mainly mediated by another intracellular messenger in rPAR1-Sf9 cells, or simply that the  $\text{PLC}\beta$  in insect cells is insensitive to D-609.

In mammalian cells, PAR1 is also known to couple to the  $\text{G}\alpha_i$  pathway. The activation of  $\text{G}\alpha_i$  is known to inhibit AC and subsequent PKA [26]. The  $\text{G}_i$ -PKA pathway is involved in downstream MAPK activation in mammalian cell studies, however, limited studies have been conducted to study the intermediate steps in the PKA pathway in Sf9 cells [40]. Furthermore, insect cell  $\text{G}\alpha_i$  does not couple to most mammalian GPCR [40].

In the current study, PKA inhibition with H-89 was used to explore the role of PKA as a contributor to the  $\text{Ca}^{2+}$  signal. The results obtained with this agent, i.e., the suppression of a  $\text{Ca}^{2+}$  flux in  $\text{Ca}^{2+}$ -free medium, suggest that PKA is critical to the  $\text{Ca}^{2+}$  mobilization from intracellular storage sites. H-89 was initially thought to inhibit PKA by competitively binding

to the ATP binding site of this kinase, thereby interfering with its phosphorylation and activation. However, H-89 has recently been found to also interfere with  $K^+$  and  $Ca^{2+}$  channels [37], although how it does so remains unclear, and no such results have been detected in Sf9 cells. H-89 has also been shown to affect other PKA-dependent factors, including the  $Ca^{2+}$ -ATPase, an essential component to  $Ca^{2+}$  storage in the ER [84].

In the rPAR1-Sf9 system, it is possible that H-89 was strictly acting on PKA, suggesting that the PKA-cAMP pathway is a critical cofactor in the release of  $Ca^{2+}$  from the ER, primarily in a  $Ca^{2+}$  deficient environment where intracellular storage sites are the only source of  $Ca^{2+}$ .

The uncertainty with regards to the exact role H-89 exerts in the rPAR1-Sf9 system makes it impossible to determine how H-89 acts in Sf9 cells and whether PKA has a definite role in the  $Ca^{2+}$  signal in rPAR1-Sf9. In the event that H-89 interferes directly with the  $Ca^{2+}$  channels [37], this would be highly revealing as to the critical role of  $Ca^{2+}$  channels in regulating the release of  $Ca^{2+}$  from the ER, as suggested by the results in  $Ca^{2+}$ -free environment, as well as being further supported by the findings with D-600.

D-600 is a lipophilic calcium-channel blocker which can exert its activity intracellularly, as well as extracellularly. In this work, D-600 could abolish the PAR1-AP induced response in a  $Ca^{2+}$  free environment. The reason for this is unclear but may suggest that D-600's action on intracellular  $Ca^{2+}$  channel blockade prevented  $Ca^{2+}$  release from intracellular storage sites. These findings may, alternately, suggest that functional  $Ca^{2+}$  channels are required for the PAR1-AP response to occur.

The ability of D-600 to induce  $Ca^{2+}$  oscillations in calcium-rich media suggests that this lipophilic agent also interfered with  $Ca^{2+}$  resequestration following the plateau phase.

The interference by D-600, therefore, may have occurred in both the efflux of  $\text{Ca}^{2+}$  from storage sites into the cytosolic space and the resequestration of  $\text{Ca}^{2+}$  into the ER.

### 4.3 Store-operated $\text{Ca}^{2+}$ entry

While previous studies have demonstrated the successful expression and functional coupling of PAR1 in Sf9 cells [82], this study is the first demonstration of intracellular  $\text{Ca}^{2+}$  signalling in response to PAR1 activating peptides in single PAR1 expressing Sf9 cells.

Sf9 cells are known to have the molecular machinery necessary for receptor-mediated  $\text{Ca}^{2+}$  signalling. They possess effective G-protein coupled  $\text{Ca}^{2+}$  signalling which accesses thapsigargin-sensitive  $\text{Ca}^{2+}$  stores [40].

Thapsigargin promotes  $\text{Ca}^{2+}$ -store depletion through its inhibition of  $\text{Ca}^{2+}$ -ATPase [70]. Consistent with previous studies, thapsigargin acted to mobilize the  $\text{Ca}^{2+}$  from the ER, causing a small transient increase in the  $[\text{Ca}^{2+}]_i$  [85]. Furthermore, in this work, depletion of the  $\text{Ca}^{2+}$  from the ER with thapsigargin eliminated the response to PAR1-AP.

On the other hand, inhibition of the  $\text{Ca}^{2+}$  release from intracellular sequestration sites, with TMB-8, inhibited the PAR1-AP effect in 50% of the rPAR1 expressing cells tested. The effect of TMB-8 was most notable in the absence of extracellular  $\text{Ca}^{2+}$  where 100% of the cells tested showed inhibition of the calcium transient produced by PAR1-AP. The reason for this inconsistent effect is not entirely clear. However, it could suggest that while in 0GSM the  $\text{Ca}^{2+}$  surge is only due to release of  $\text{Ca}^{2+}$  from storage sites, in 2.8GSM, the source of  $\text{Ca}^{2+}$  is a combination of release from intracellular sites and entry from the extracellular space.

Altogether, these results suggest that the primary phase of the PAR1-AP-induced  $[\text{Ca}^{2+}]_i$  response in rPAR1-Sf9 cells is dependent on the release of  $\text{Ca}^{2+}$  from intracellular storage sites following the addition of PAR1-AP and can be inhibited by either depleting the

Ca<sup>2+</sup> storage site with thapsigargin or preventing the release of Ca<sup>2+</sup> from these sites with TMB-8.

Interestingly, assays conducted with the lipophilic voltage-dependent Ca<sup>2+</sup> channel blocker D-600 could add information regarding the contribution of extracellular Ca<sup>2+</sup> to the primary phase of the PAR1-AP response. D-600 demonstrated that functional Ca<sup>2+</sup> channels are required in order for the first phase of the PAR1-AP response to be produced.

When taken altogether, results obtained in calcium-rich and calcium-free media demonstrated that the PAR1-AP response possesses two phases to the Ca<sup>2+</sup> flux. The results suggest an initial release of Ca<sup>2+</sup> from internal stores and a subsequent influx of Ca<sup>2+</sup> dependent on the initial release.

Currently available evidence suggests that Sf9 cells possess endogenous voltage-gated Ca<sup>2+</sup> channels [40, 62], as well as a component of calcium entry known as store-operated calcium entry (SOCE) [70].

As the name implies, the activation of store-operated calcium channels (SOC) occurs after the initial release of Ca<sup>2+</sup> from intracellular stores, thus following Ca<sup>2+</sup> store depletion [39]. Ca<sup>2+</sup> stores are able to transmit store depletion to the plasma membrane and the extracellular space, leading to the activation of a Ca<sup>2+</sup> entry system. This transmission of information related to Ca<sup>2+</sup> storage levels is thought to occur through stromal interacting molecule-1 (STIM-1) [38]. STIM-1 resides on the luminal surface of the ER and serves as a detector of low levels of Ca<sup>2+</sup>. This causes the translocation of STIM-1 to the ER-plasma membrane junctions, known as puncta. Once translocated to the puncta, STIM-1 interacts with store operated Ca<sup>2+</sup> (SOC) channels on the plasma membrane, thereby critically mediating their activity [39].

There are two types of SOC; the first of these is the Orai-1, a  $\text{Ca}^{2+}$ -selective channel which functions as an L-type  $\text{Ca}^{2+}$  channel. The second type is the transient receptor potential (Trp) channel, a non-selective cation channel [38, 39].

In previous studies using cell suspensions, and conducted by microspectrofluoroscopy, it was concluded that the octopamine response primarily reflects  $\text{Ca}^{2+}$  release from internal stores [70]. A secondary influx of  $\text{Ca}^{2+}$  from the extracellular space was also detected in response to octopamine stimulation [70]. The current study demonstrates, for the first time, that an exogenous receptor expressed in Sf9 cells is able to activate SOCE.

These findings are supported by the results obtained using both  $\text{La}^{3+}$  and nifedipine which eliminate the plateau phase of the PAR1-AP response in rPAR1-Sf9 cells, suggesting the need for  $\text{Ca}^{2+}$  entry from the extracellular space.

The detection of a  $\text{Ca}^{2+}$  influx related to SOC channels in Sf9 cells has been very limited [70]. While it has previously been described that recombinant baculovirus infection of Sf9 cells can induce a slight change in the membrane permeability to  $\text{Ca}^{2+}$  by activating a cation channel [62], later work has suggested a directly activated  $\text{Ca}^{2+}$  channel in Sf9 cells expressing the  $M_5$  muscarinic receptors [70] but not when expressing other exogenous proteins. The reason for limited detection of SOC activity in Sf9 using recombinant baculovirus may also be explained in part by findings relevant to mammalian cells. Interestingly, studies conducted using mammalian cells have suggested that store-operated  $\text{Ca}^{2+}$  entry (SOCE) was only associated with a portion of the  $\text{Ca}^{2+}$  stores and contributes to the amplification of the peak  $\text{Ca}^{2+}$  signal above that achieved by  $\text{Ca}^{2+}$  release alone [86, 87]. Specifically, only a subset or fraction of the  $\text{Ca}^{2+}$  release from  $\text{Ca}^{2+}$  stores contributes to the translocation of STIM-1 to the puncta, and activation of SOCE [86, 88]. STIM-1 has been

shown to be activated when store concentration levels reach a very low threshold  $\text{Ca}^{2+}$  level [38]. A similar, distinct, subset of  $\text{Ca}^{2+}$  stores has been detected in Sf9 cells [70]. It is possible that  $\text{Ca}^{2+}$ -store depletion following octopamine, or following activation of other recombinant receptors expressed in Sf9 cells do not drain  $\text{Ca}^{2+}$  stores enough to reach threshold levels of  $\text{Ca}^{2+}$  required for STIM-1 translocation and SOCE activation.

The variable coupling ability of exogenous receptors to the Sf9 signalling apparatus cannot be ruled out as a potential reason for the failure to access the SOCE-specific subset of  $\text{Ca}^{2+}$  stores in Sf9 cells.

In summary, the data obtained in this study suggests, for the first time, a role for a SOCE activation following exogenous receptor activation in Sf9 cells.



## **CONCLUSION AND FUTURE DIRECTIONS**

## 5.1 Conclusion

The current study set out to determine whether recombinant baculovirus expression using Sf9 cells could effectively express functional rPAR1 capable of coupling to the Sf9 cells signalling apparatus.

The study of distinct receptors in mammalian cells can be difficult for several reasons and can be circumvented by using the recombinant baculovirus-Sf9 signalling system. For instance, mammalian cells may contain lower receptor densities than can be achieved in a recombinant expression system. From a receptor activation perspective, multiple receptors or receptor subtypes may exist, with similar ligand binding properties [89]. Lastly, receptor cross-talk cannot be ruled out when trying to study receptor-mediated responses in mammalian cells [89-91].

Data obtained through the current study confirms the utility of the Sf9-recombinant baculovirus expression system as a versatile heterologous expression system. While some limitations exist, this system allowed for the selective expression of a mammalian protein highly similar to the native protein. rPAR1 was localized mainly at the cell surface and was able to maintain its native agonist specificity.

rPAR1 was also shown to couple effectively with the insect cell signalling apparatus, both in response to thrombin and PAR1-AP. Receptor activation was able to produce a downstream signal which was studied using a variety of signal modulators and channel blockers.

Signal modulators suggest a critical role for PKC in the rPAR1-Sf9  $\text{Ca}^{2+}$  response.

This  $\text{Ca}^{2+}$  response, measured using Fura-2, is composed of two phases. The first phase of the response is mediated by PKC, and requires the presence of functional  $\text{Ca}^{2+}$

channels, particularly intracellularly, for the initial release of  $\text{Ca}^{2+}$  from  $\text{Ca}^{2+}$  stores. This release of  $\text{Ca}^{2+}$  from the ER is critically regulated by low levels of PKC, presumably since high levels of PKC may cause early phosphorylation of the PAR1 and receptor deactivation, as well as the phosphorylation of  $\text{IP}_3\text{R}$  and  $\text{Ca}^{2+}$  channels, essentially causing them to become inactivated faster .

The second phase of the  $\text{Ca}^{2+}$  response in rPAR1-Sf9 cells involves activation of store-operated  $\text{Ca}^{2+}$  entry not previously described with PAR1 expression.

## **5.2 Future directions**

The Sf9-baculovirus expression system is a useful expression system to study the expression and functional coupling of rPAR1. However, the pathological state resulting from infection with the baculovirus results in the questionable dependability of this expression system. A stably transfected Sf9 cell line, capable of expressing a functional receptor, could provide a more reliable system to study receptor activation and the Sf9 cell could provide an isolated environment to study a selected mammalian receptor such as the rPAR1. This system could also be a method of choice for the study of orphan receptors, and screening of compound libraries.

Ultimately, an exogenous ligand, capable of selectively activating/inactivating a signalling pathway, could be developed to modulate thrombin's cell-targeted activities.

The potential therapeutic usefulness of inhibiting PAR1 has led to the development of several PAR1 receptor antagonists studied for their potential in the long-term prevention of cardiovascular events including myocardial infarct, cardiovascular death and stroke.

## **APPENDIX**

### **Calibration of intracellular $\text{Ca}^{2+}$ concentration**

The calibration procedure consisted of the addition of 10 $\mu$ M ionomycin to a wild-type Sf9 cell bathing in a 10mM Ca<sup>2+</sup> medium, causing the intracellular [Ca<sup>2+</sup>] to reach the same level as its surroundings. Subsequently, a 10mM EGTA solution is added to the preparation. The resulting chelation of calcium is demonstrated by a sharp change in the fluorescence being emitted. This experiment allows us to relate the observed calcium response, resulting from cell stimulation, to the maximal and minimal observable signal in the Sf9 cell type. This allows us to draw a link between the fluorescence ratio and the quantitative change in the intracellular [Ca<sup>2+</sup>].

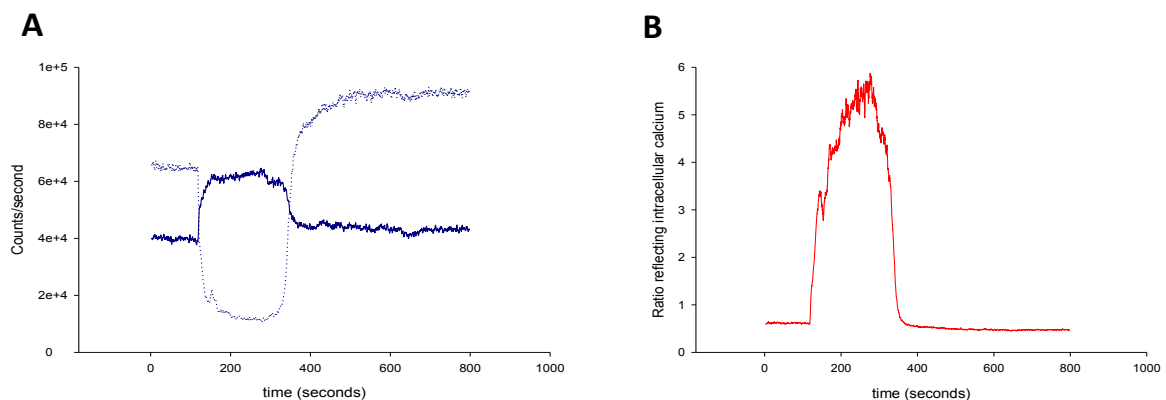


**Figure 25: Calibration of the Sf9 calcium signal. A: Individual tracings.** Tracings obtained using dual excitation at wavelengths of 340 and 380nm for a single Sf9 cell in 10mM Ca<sup>2+</sup> solution. The addition of 10 $\mu$ M ionomycin followed by 10mM EGTA in Ca<sup>2+</sup>-free solution occurred at 127 seconds and 280 seconds, respectively. **B: Ratio representative of the calibration of the Sf9 Ca<sup>2+</sup> signal.** Normalized ratio  $F_{340}/F_{380}$  shown is representative of results obtained for 3 identical experiments.

The maximum and minimum measurable ratio reflecting [Ca<sup>2+</sup>]<sub>i</sub> can be determined.

The ratio value was used to determine the cellular response to changes in [Ca<sup>2+</sup>]<sub>i</sub>.

Calculation of  $[Ca^{2+}]_i$  can be performed using the following formula based on the value of the ratio [92]:

$$[Ca^{2+}]_i = K_d (R - R_{min}/R_{max} - R) \times F_{0\ 380} / F_{S\ 380}$$

where  $K_d$  represents a constant,  $R_{min}$  and  $R_{max}$  are the minimum and maximum observable  $Ca^{2+}$  ratios and  $F_{0\ 380} / F_{S\ 380}$  represents the fluorescent values in a calcium-free and calcium-saturated solutions at 380nm wavelength.

The equation can be simplified by adding in the value of the constant for  $K_d$  equal to 135mM at room temperature, and the values obtained through the calibration experiment, as shown on Figure 23B:

$$[Ca^{2+}]_i = 135mM (R - 0.49/5.26 - R) \times 7.33$$

## **BIBLIOGRAPHY**

1. Hirano, K., *The roles of proteinase-activated receptors in the vascular physiology and pathophysiology*. *Arterioscler Thromb Vasc Biol*, 2007. **27**(1): p. 27-36.
2. Wojtukiewicz, M.Z., et al., *Thrombin increases the metastatic potential of tumor cells*. *Int J Cancer*, 1993. **54**(5): p. 793-806.
3. Vu, T.-K.H., et al., *Molecular cloning of a functional thrombin receptor reveals a novel proteolytic mechanism of receptor activation*. *Cell*, 1991. **64**(6): p. 1057-1068.
4. Macfarlane, S.R., *Proteinase-Activated Receptors*. *Pharmacol Rev*, 2001. **53**(2): p. 246-283.
5. Pawlinski, R. and M. Holinstat, *We Can Do It Together: PAR1/PAR2 Heterodimer Signaling in VSMCs*. *Arterioscler Thromb Vasc Biol*, 2011. **31**(12): p. 2775-6.
6. Ramachandran, R. and M.D. Hollenberg, *Proteinases and signalling: pathophysiological and therapeutic implications via PARs and more*. *Br J Pharmacol*, 2008. **153**(S1): p. S263-82.
7. Tracy, R.P., *Thrombin, inflammation, and cardiovascular disease: an epidemiologic perspective*. *Chest*, 2003. **124**(3 Suppl): p. 49S-57S.
8. Coughlin, S.R., *Protease-activated receptors in hemostasis, thrombosis and vascular biology*. *Thromb Haemost*, 2005. **3**: p. 14.
9. Coughlin, S.R., *Thrombin signalling and protease-activated receptors*. *Nature*, 2000. **407**: p. 6.
10. Gandhi, P.S., et al., *Structural identification of the pathway of long-range communication in an allosteric enzyme*. *Proc Natl Acad Sci U S A*, 2008. **105**(6): p. 1832-7.
11. Guillin, M.C., et al., *Thrombin specificity*. *Thromb Haemost*, 1995. **74**(1): p. 129-33.
12. Zhang, C., et al., *High-resolution crystal structure of human protease-activated receptor 1*. *Nature*, 2012. **advance online publication**.
13. Zhang, C., *High-resolution crystal structure of human protease-activated receptor 1*. *Nature*, 2012. **492**(20 Dec 2012): p. 8.
14. Grand, R.J., A.S. Turnell, and P.W. Grabham, *Cellular consequences of thrombin-receptor activation*. *Biochem J*, 1996. **313 ( Pt 2)**: p. 353-68.
15. Seeley, S., *Structural basis for thrombin activation of a protease-activated receptor: inhibition of intramolecular liganding*. *Chem Biol*, 2003. **10**(11): p. 1033-41.
16. Edelman, L., et al., *Obtaining a functional recombinant anti-rhesus (D) antibody using the baculovirus-insect cell expression system*. *Immunology*, 1997. **91**(1): p. 13-9.
17. Ishii, K., et al., *Determinants of thrombin receptor cleavage. Receptor domains involved, specificity, and role of the P3 aspartate*. *J Biol Chem*, 1995. **270**(27): p. 16435-40.
18. Frost, G.H., J.S. Bergmann, and D.H. Carney, *Glycosylation of high-affinity thrombin receptors appears necessary for thrombin binding*. *Biochem Biophys Res Commun*, 1991. **180**(1): p. 349-55.
19. Bahou, W.F., et al., *Identification of a novel thrombin receptor sequence required for activation-dependent responses*. *Blood*, 1994. **84**(12): p. 4195-202.
20. Troyer, D., et al., *Stimulation of the thrombin receptor of human glomerular mesangial cells by Ser-Phe-Leu-Leu-Arg-Asn-Pro-Asn-Asp-Lys-Tyr-Glu-Pro-Phe peptide*. *J Biol Chem*, 1992. **267**(28): p. 20126-31.
21. Nystedt, S., et al., *Molecular Cloning and Functional Expression of the Gene Encoding the Human Proteinase-Activated Receptor 2*. *J Biol Chem*, 1995. **270**: p. 5950-5955.



22. Ishihara, H., et al., *Protease-activated receptor 3 is a second thrombin receptor in humans*. Nature, 1997. **386**(6624): p. 502-6.
23. Kahn, M.L., et al., *Protease-activated receptors 1 and 4 mediate activation of human platelets by thrombin*. J Clin Invest, 1999. **103**(6): p. 879-87.
24. Schmidt, V.A., et al., *The human thrombin receptor and proteinase activated receptor-2 genes are tightly linked on chromosome 5q13*. Br J Haematol, 1997. **97**(3): p. 523-9.
25. Xu, W.F., et al., *Cloning and characterization of human protease-activated receptor 4*. Proc Natl Acad Sci U S A, 1998. **95**(12): p. 6642-6.
26. Barr, A.J., L.F. Brass, and D.R. Manning, *Reconstitution of receptors and GTP-binding regulatory proteins (G proteins) in Sf9 cells. A direct evaluation of selectivity in receptor.G protein coupling*. J Biol Chem, 1997. **272**(4): p. 2223-9.
27. Hollenberg, M.D. and S.J. Compton, *International Union of Pharmacology. XXVIII. Proteinase-activated receptors*. Pharmacol Rev, 2002. **54**(2): p. 203-17.
28. Bourne, H.R., *How receptors talk to trimeric G proteins*. Curr Opin Cell Biol, 1997. **9**(2): p. 134-42.
29. Offermanns, S., et al., *G proteins of the G12 family are activated via thromboxane A2 and thrombin receptors in human platelets*. Proc Natl Acad Sci U S A, 1994. **91**(2): p. 504-8.
30. Macfarlane, S.R., et al., *The role of intracellular Ca<sup>2+</sup> in the regulation of proteinase-activated receptor-2 mediated nuclear factor kappa B signalling in keratinocytes*. Br J Pharmacol, 2005. **145**(4): p. 535-44.
31. Hassock, S.R., et al., *Expression and role of TRPC proteins in human platelets: evidence that TRPC6 forms the store-independent calcium entry channel*. Blood, 2002. **100**(8): p. 2801-11.
32. Ogawa, H., et al., *The thrombin receptor transmits signals through a 33-kDa protein kinase in human platelets*. Biochem Biophys Res Commun, 1994. **203**(2): p. 907-13.
33. Foskett, J.K., et al., *Inositol Trisphosphate Receptor Ca<sup>2+</sup> Release Channels Ion Channels*. Physiol Rev, 2007. **87**(2): p. 593-658.
34. Monette, R., et al., *Interaction between Calcium Ions and Bacillus thuringiensis Toxin Activity against Sf9 Cells (Spodoptera frugiperda, Lepidoptera)*. Appl Environ Microbiol, 1997. **63**(2): p. 440-7.
35. Jetley, M. and A.H. Weston, *Some effects of D600, nifedipine and sodium nitroprusside on electrical and mechanical activity in rat portal vein [proceedings]*. Br J Pharmacol, 1976. **58**(2): p. 287P-288P.
36. Dolan, A., *Systems modeling of Ca<sup>2+</sup> homeostasis and mobilisation in platelets mediated by IP3 and store-operated Ca<sup>2+</sup> entry*. Biophysical Journal, 2014. **106**(May 2014): p. 12.
37. Murray, A. *Pharmacological PKA inhibition: All may not be what it seems*. Science Signaling, 2008. **1** (22), pg. re4.
38. Abramowitz, J., *TRP Ion Channel Function in Sensory Transduction and Cellular Signaling Cascades*. NCBI Bookshelf, ed. W. Liedtke, Heller S. 2007, Boca Raton: CRC Press.
39. Moreno, C., *SOC AND NOW ALSO SIC: Store-operated and Store-inhibited Channels*. Life, 2011. **63**(10): p. 7.

40. Schneider, E.H. and R. Seifert, *Sf9 cells: a versatile model system to investigate the pharmacological properties of G protein-coupled receptors*. *Pharmacol Ther*, 2010. **128**(3): p. 387-418.
41. Kawasaki, T., et al., *Protein kinase C-induced phosphorylation of Orail regulates the intracellular Ca<sup>2+</sup> level via the store-operated Ca<sup>2+</sup> channel*. *J Biol Chem*, 2010. **285**(33): p. 25720-30.
42. Politi, A., et al., *Models of IP<sub>3</sub> and Ca<sup>2+</sup> Oscillations: Frequency Encoding and Identification of Underlying Feedbacks*. *Biophys J*, 2006. **90**(9): p. 3120-33.
43. Toullec, D., et al., *The bisindolylmaleimide GF 109203X is a potent and selective inhibitor of protein kinase C*. *J Biol Chem*, 1991. **266**(24): p. 15771-81.
44. Gao, Y., et al., *Role of protein kinase C in the activation of store-operated Ca(2+) entry in airway smooth muscle cells*. *J Huazhong Univ Sci Technolog Med Sci*, 2012. **32**(3): p. 303-10.
45. Ishii, K., et al., *Inhibition of thrombin receptor signaling by a G-protein coupled receptor kinase. Functional specificity among G-protein coupled receptor kinases*. *J Biol Chem*, 1994. **269**(2): p. 1125-30.
46. Hoxie, J.A., et al., *Internalization and recycling of activated thrombin receptors*. *J Biol Chem*, 1993. **268**(18): p. 13756-63.
47. Brass, L.F., et al., *Thrombin receptors: turning them off after turning them on*. *Semin Hematol*, 1994. **31**(3): p. 251-60.
48. Hein, L., et al., *Intracellular targeting and trafficking of thrombin receptors. A novel mechanism for resensitization of a G protein-coupled receptor*. *J Biol Chem*, 1994. **269**(44): p. 27719-26.
49. Schuepbach, R.A. and M. Riewald, *Coagulation factor Xa cleaves protease-activated receptor-1 and mediates signaling dependent on binding to the endothelial protein C receptor*. *J Thromb Haemost*, 2010. **8**(2): p. 379-88.
50. Kuliopulos, A., et al., *Plasmin desensitization of the PAR1 thrombin receptor: kinetics, sites of truncation, and implications for thrombolytic therapy*. *Biochemistry*, 1999. **38**(14): p. 4572-85.
51. Abdallah, R.T., et al., *Plasma kallikrein promotes epidermal growth factor receptor transactivation and signaling in vascular smooth muscle through direct activation of protease-activated receptors*. *J Biol Chem*, 2010. **285**(45): p. 35206-15.
52. Oikonomopoulou, K., et al., *Kallikrein-mediated cell signalling: targeting proteinase-activated receptors (PARs)*. *Biol Chem*, 2006. **387**(6): p. 817-24.
53. Mosnier, L.O., et al., *Biased agonism of protease-activated receptor 1 by activated protein C caused by noncanonical cleavage at Arg46*. *Blood*, 2012. **120**(26): p. 5237-46.
54. Goerge, T., et al., *Tumor-derived matrix metalloproteinase-1 targets endothelial proteinase-activated receptor 1 promoting endothelial cell activation*. *Cancer Res*, 2006. **66**(15): p. 7766-74.
55. Mihara, K., et al., *Neutrophil elastase and proteinase-3 trigger G protein-biased signaling through proteinase-activated receptor-1 (PAR1)*. *J Biol Chem*, 2013. **288**(46): p. 32979-90.
56. Gieseler, F., et al., *Proteinase-activated receptors (PARs) - focus on receptor-receptor-interactions and their physiological and pathophysiological impact*. *Cell Commun Signal*, 2013. **11**: p. 86.

57. Gesty-Palmer, D. and L.M. Luttrell, *Heptahelical terpsichory. Who calls the tune?* J Recept Signal Transduct Res, 2008. **28**(1-2): p. 39-58.
58. Kaneider, N.C., et al., '*Role reversal*' for the receptor *PAR1* in sepsis-induced vascular damage. Nat Immunol, 2007. **8**(12): p. 1303-12.
59. Matsuura, Y., et al., *Baculovirus expression vectors: the requirements for high level expression of proteins, including glycoproteins.* J Gen Virol, 1987. **68 (Pt 5)**:p.1233-50.
60. Vialard, J.E., B.M. Arif, and C.D. Richardson, *Introduction to the molecular biology of baculoviruses.* Methods Mol Biol, 1995. **39**: p. 1-24.
61. Gerhardt, C.C., *Molecular Cloning and Pharmacological Characterization of a Molluscan Octopamine Receptor.* Molecular Pharmacology, 1997. **51**: p. 293-300.
62. Perez, J.F., et al., *Characterization of a membrane calcium pathway induced by rotavirus infection in cultured cells.* J Virol, 1999. **73**(3): p. 2481-90.
63. Barr, A.J. and D.R. Manning, *Agonist-independent activation of Gz by the 5-hydroxytryptamine1A receptor co-expressed in Spodoptera frugiperda cells. Distinguishing inverse agonists from neutral antagonists.* J Biol Chem, 1997. **272**(52): p. 32979-87.
64. Zhong, C., et al., *Molecular cloning of the rat vascular smooth muscle thrombin receptor. Evidence for in vitro regulation by basic fibroblast growth factor.* J Biol Chem, 1992. **267**(24): p. 16975-9.
65. Vouret-Craviari, V., et al., *Post-translational and activation-dependent modifications of the G protein-coupled thrombin receptor.* J Biol Chem, 1995. **270**(14): p. 8367-72.
66. Amos, W.B., J.G. White, and M. Fordham, *Use of confocal imaging in the study of biological structures.* Appl Opt, 1987. **26**(16): p. 3239-43.
67. White, J.G., W.B. Amos, and M. Fordham, *An evaluation of confocal versus conventional imaging of biological structures by fluorescence light microscopy.* J Cell Biol, 1987. **105**(1): p. 41-8.
68. Trogadis, J.E., et al., *Dopamine D1 receptor distribution in Sf9 cells imaged by confocal microscopy: a quantitative evaluation.* J Histochem Cytochem, 1995. **43**(5): p. 497-506.
69. Orr, N., *The Sf9 cell line as a model for studying insect octopamine-receptors.* Insect Biochemistry and Molecular Biology, 1992. **22**(6): p. 6.
70. Hu, Y., L. Rajan, and W.P. Schilling, *Ca<sup>2+</sup> signaling in Sf9 insect cells and the functional expression of a rat brain M5 muscarinic receptor.* Am J Physiol, 1994. **266**(6 Pt 1): p. C1736-43.
71. M, J., *Some effects of D600, nifedipine and sodium nitroprusside on electrical and mechanical activity in rat portal vein (proceedings).* British Journal of Pharmacology, 1976. **58**(2): p. 287P-288P.
72. Díaz, Y., et al., *Expression of Nonstructural Rotavirus Protein NSP4 Mimics Ca<sup>2+</sup> Homeostasis Changes Induced by Rotavirus Infection in Cultured Cells* ∇. J Virol, 2008. **82**(22): p. 11331-43.
73. Muller-Decker, A., *Interruption of TPA-induced signals by an antiviral and antitumoral xanthate compound: Inhibition of a phospholipase C-type reaction.* Biochem Biophys Res Commun, 1989. **162**(1): p. 6.
74. Mattiazzi, A., L. Hove-Madsen, and D.M. Bers, *Protein kinase inhibitors reduce SR Ca transport in permeabilized cardiac myocytes.* Am J Physiol, 1994. **267**(2 Pt 2): p. H812-20.

75. Schneider, E.H. and R. Seifert, *Coexpression systems as models for the analysis of constitutive GPCR activity*. Methods Enzymol, 2010. **485**: p. 527-57.
76. Raming, K., *Cloning and expression of odorant receptors*. Nature Lond, 1993. **361**: p. 4.
77. McLachlin, J.R., *Stable transformation of insect cells coexpress a rapidly selectable marker gene and an inhibitor of apoptosis*. In Vitro Cellular Development and Biology - Animal, 1997. **33**(July-August): p. 4.
78. Ishii, K., et al., *Kinetics of thrombin receptor cleavage on intact cells. Relation to signaling*. J Biol Chem, 1993. **268**(13): p. 9780-6.
79. Trejo, J., S.R. Hammes, and S.R. Coughlin, *Termination of signaling by protease-activated receptor-1 is linked to lysosomal sorting*. Proc Natl Acad Sci U S A, 1998. **95**(23): p. 13698-702.
80. Trejo, J., *Protease-Activated Receptors: New concepts in Regulation of G Protein-coupled receptor signaling and Trafficking*. The Journal of Pharmacology and Experimental Therapeutics, 2003. **307**(2): p. 5.
81. Henrikson, K.P., *Expression of rat thrombin receptor and mutants in the baculovirus-infected insect cell system*. Thrombosis Research, 1997. **87**(2): p. 9.
82. Chen, X., et al., *Functional expression of a human thrombin receptor in Sf9 insect cells: evidence for an active tethered ligand*. Biochem J, 1996. **314** ( Pt 2): p. 603-11.
83. McCoy, K.L., S.F. Traynelis, and J.R. Hepler, *PAR1 and PAR2 Couple to Overlapping and Distinct Sets of G Proteins and Linked Signaling Pathways to Differentially Regulate Cell Physiology*. Mol Pharmacol, 2010. **77**(6): p. 1005-15.
84. Hussain, M., et al., *Effects of the protein kinase A inhibitor H-89 on Ca<sup>2+</sup> regulation in isolated ferret ventricular myocytes*. Pflugers Arch, 1999. **437**(4): p. 529-37.
85. Tian, P., et al., *The nonstructural glycoprotein of rotavirus affects intracellular calcium levels*. J Virol, 1994. **68**(1): p. 251-7.
86. Harper, M., *Store-operated calcium entry and non-capacitative calcium entry have distinct roles in thrombin-induced calcium signalling in human platelets*. Cell Calcium, 2011. **50**: p. 7.
87. Jardin, I., *Intracellular calcium release from human platelets: Different messengers for multiple stores*. Trends Cardiovasc Med, 2008. **18**: p. 9.
88. Flemming, R., *Discrete store-operated calcium influx into an intracellular compartment in rabbit arteriolar smooth muscle*. Journal of Physiology, 2002. **543**.2: p. 11.
89. O'Brien, P.J., et al., *Thrombin responses in human endothelial cells. Contributions from receptors other than PAR1 include the transactivation of PAR2 by thrombin-cleaved PAR1*. J Biol Chem, 2000. **275**(18): p. 13502-9.
90. Shankar, H., et al., *P2Y12 receptor-mediated potentiation of thrombin-induced thromboxane A2 generation in platelets occurs through regulation of Erk1/2 activation*. J Thromb Haemost, 2006. **4**(3): p. 638-47.
91. Wu, C.C., et al., *The roles and mechanisms of PAR4 and P2Y12/phosphatidylinositol 3-kinase pathway in maintaining thrombin-induced platelet aggregation*. Br J Pharmacol, 2010. **161**(3): p. 643-58.
92. Grynkiewicz, G., M. Poenie, and R.Y. Tsien, *A new generation of Ca<sup>2+</sup> indicators with greatly improved fluorescence properties*. J Biol Chem, 1985. **260**(6): p. 3440-50.